PARTICLE BEHAVIOR IN FLOW THROUGH SMALL BIFURCATIONS

by

Robert LEVINE

A thesis submitted to the Faculty of Graduate Studies and Research of McGill University in partial fulfilment of the requirements for the degree of

Master of Engineering

Department of Chemical Engineering,
McGill University,
Montreal, Quebec.

January, 1977.

ABSTRACT

Atherosclerotic plaques and platelet thrombi have been observed downstream of bifurcations in the cardiovascular system of man and animals where flow separation and vortex formation can occur. Hence, studies of particle flow behavior in dissected, fixed and mounted dog -mesentery bifurcations and small model Y- and T-bifurcations were carried out.

Using suspensions of rigid spheres $\leq$ 35 μm diameter, no separation of streamlines was found in the mesentery bifurcations, even at the highest Reynolds numbers. In model Y-bifurcations, having lower radii of curvature, a secondary crossflow and eventual flow separation was observed. Particles moved laterally across the streamlines of the primary flow and entered spiral vortices at the outer wall of the hips of the bifurcation.

Flow in a symmetric, partially obstructed T-bifurcation was also studied and a spiral vortex observed at the entry of the obstructed daughter branch.

RESUME

On a observé des plaques artériosclérotiques et des thrombi plaquettaires aux bifurcations du système cardiovasculaire chez l'homme et chez les animaux, où on trouve une séparation de l'écoulement et où une formation de tourbillons se produisent. Pour mieux comprendre les mécanismes en cause, on a étudié le comportement des particules en écoulement dans les bifurcations mésentériques disséqués, et sur des modèles réduits des bifurcations de formes "Y" et "T". Même au nombre de Reynolds le plus élevé, où nous avons utilisé des sphères rigides en suspension, aucune séparation d'écoulement n'a été observé dans ces bifurcations mésentériques. Dans les modèles de bifurcations de forme "Y", démontrés comme ayant un rayon de courbure réduit et où un contre écoulement secondaire a lieu, une séparation de l'écoulement est observée. Dans ce cas, les particules se déplacent latéralement à travers les axes d'écoulement primaire et engendrent des mouvements de spirales vers les paroies extérieures.

L'écoulement dans une bifurcation symmetrique partiallement obstruée, fut egalement étudié; on y observé un mouvement de tourbillon à l'entrée de l'embranchement obstruée.

ACKNOWLEDGMENTS

The author wishes to express his sincere graditude to his thesis supervisor Dr. H.L. Goldsmith for his guidance, help and support during the course of this work, especially in the preparation of the thesis.

The author is also grateful to the Quebec Heart Foundation for their financial support of this project.

Thanks are also due to Dr. W.A. Mersereau for his time, advice and help in the preparation of the dog mesentery bifurcations.

The author would like to thank Mr. A. Hageman and Mr. A. Kluck for constructing the model flow systems.

Mr. T. Karino and Dr. A.S. Mujumdar of the Department of Chemical Engineering at McGill University are gratefully acknowledged for their advice and readiness to discuss problems.

Many thanks are given to Ms. D. Chajczyk for her technical assistance and help in the final preparations of the thesis.

Ms. P. MacDougall is especially thanked for her skillful and artistic preparation of the figures and graphs.

Ms. P. Spicer of the Dept. of Pathology at the Montreal General Hospital is acknowledged for her advice in the fixing of the dog mesentery bifurcations and her preparations of the serial sections.

A very special thanks to my wife, Risë, for her patience, care and encouragement during the many months of this work.

Finally, I would like to express my thanks to Ms. N. Armstrong and Ms. P. Lilley for their careful diligent typing of this thesis.

FOREWORD

This thesis describes the behavior of model particles in flow through bifurcations resembling those found in the vasculature of man.

The main portion of the thesis, Chapter II, has been written as a self contained work in a manner suitable for publication in the scientific literature with little further modification. Thus, Chapter II contains its own Introduction, List of Symbols, Experimental Part, Results, Discussion and Bibliography. This has necessitated the ommission of details of the experimental apparatus and calculations which are therefore given in Appendices A and B respectively.

A review of the general background and the scope of the thesis is given in Chapter I.

TABLE OF CONTENTS

Figure | Page

LIST OF FIGURES

CHAPTER I

CHAPTER II

APPENDIX A

Table Page

LIST OF TABLES

CHAPTER II

CHAPTER I

General Introduction

This Thesis deals with the microscopic flow behavior of spherical particles in dilute suspensions moving through bifurcations similar to those found in the vasculature of man and animals. Since cardiovascular diseases, amongst them atherosclerosis and thrombosis, are responsible for more deaths among North American men than any other, biomedical researchers are devoting considerable time and effort to understand the occurrence and development of these diseases. The scientific literature abounds with papers dealing with the biochemical, physiological, and pathological aspects of these cardiovascular disorders, but certain aspects of these diseases are still poorly understood. Here, we are concerned with the effects of blood flow on the development of arterial thrombosis. It has long been suspected that fluid mechanical factors are involved in the localization of sites of injury at vessel walls and the adhesion there of platelet thrombi which can grow and eventually lead to the total occlusion of the vessel lumen. It is significant that these same sites in the arterial tree are regions where flow separation and vortex formation are likely to occur. Here, one finds the deposition of lipids, mostly cholesterol, leading to the formation of atheromatous plaques.

Among the above mentioned sites are bifurcations and T-joints in the vasculature. The experimental part of this thesis represents an initial study of flow through channels having such geometry. The first part investigates the behavior of particles flowing through small bifurcations, dissected out from the dog mesentery and subsequently fixed and mounted. These branching blood

vessels are quite similar, with respect to shape and geometry, to those in the peripheral arteries of man. It was shown that even at the highest Reynolds numbers used, flow separation and the formation of vortices did not occur. However, as described in the second part, when the radius of curvature of the outer walls of the bifurcation was decreased and the area ratio increased, flow separation and vortex formation was observed at higher Reynolds number, at the hips of the bifurcation. It is in this region that other investigators have found histological evidence of atherosclerotic lesions and the deposition of platelet thrombi. The last section of the experimental part investigates flow in a T-bifurcation and the effect of partially occluding one branch. It was found that such occlusion leads to flow separation and the formation of vortices at the entrance of the obstructed daughter branch.

(1) Atherosclerosis: Mechanisms and Localization

Atherosclerosis is a degenerative disease that affects relatively large arteries by progressive thickening and eventual hardening of the vessel wall through the formation of atheromatous plaques, usually of high lipid (cholesterol) content. It has long been known to be an underlying cause of death in persons over 50. Yet atherosclerotic lesions have been found in children, even infants, giving evidence that atherosclerosis is not only limited to old age.

Various factors are believed to affect the progress of the disease, such as lack of exercise and dietary fat content. Because experimental animals have been found to develop atherosclerotic plaques high in lipid content after being placed on a diet containing

a high cholesterol level, many researchers believe atherosclerotic lesions are derived from the insudation of plasma into the arterial wall. (Virchow, 1862; Aschoff, 1924; Anitschkow, 1933; Caro et al., 1971; Walton, 1975). This theory proposes that atherosclerotic lesions arise from altered endothelial permeability allowing plasma proteins (lipoproteins and fibrinogen) to permeate the endothelium and react with the constituents of the arterial wall. While this theory cannot account for the localization of atheroma at curved segments, expansions or constrictions, and branching blood vessels in the arterial system (Stehbens, 1960; Strong and McGill, 1962; Schwartz et al., 1967; Caro et al., 1971), some researchers have suggested that there is a causative relationship between arterial blood fluid mechanics and the development of the vessel injury (Duguid, 1926; Willis, 1954; Texon et al., 1960; Wesolowski et al., 1965; Fry, 1969). Texon et al., (1960) have hypothesized that in regions of low pressure (locally increased blood velocity) a suction force exerted on the endothelial lining causes the layer to separate from the adjacent tissue, thickening the intima and eventually leading to the formation of atheroma. However, a suction force on the endothelium will only exist if the local pressure exceeds that of the intraluminal pressure. This has been calculated to be negligible under physiological conditions. (Caro et al., 1971; Gessner, 1973).

A model proposed by Wesolowski et al., (1962, 1965) suggests that atherosclerotic lesions are formed in regions of turbulence as a result of (i) induced vibration of the arterial wall which may lead to the eventual injury of the intima, or (ii) local increases

in lateral (static) wall pressure which may injure the intima or lead to local lipid accumulation within the intima, suppression of lipid secretion from within the arterial wall or both. Whether this hypothesis is true depends upon the magnitude of the fluctuations in turbulent wall static pressure which has yet to be determined under physiological conditions (Gessner, 1963).

Another important factor is the local wall shear stress which has been implicated in bringing about damage to the endothelial wall and increasing its permeability to lipids. On the one hand, Fry (1968) has shown in vivo, that in a region of abnormally high wall shear stress (379 ± 85 dyne cm^{-2}) acute changes in endothelial histology can occur. In a later study, Fry (1969) observed that, at shear stresses below 379 dyne cm^{-2}, there is an apparent increase in wall permeability, thus implying that arterial wall damage is not necessary for an increase in the flux of lipoproteins. It was first thought that such high stresses do not exist in vivo. Thus, Ling et al., (1968) measured peak wall shear stresses in the thoracic aorta between 80 and 160 dynes cm^{-2} over a cardiac cycle. In a later study Ling et al., (1969), measured peak wall shear stresses in a distensible model of the renal artery branch under simulated in vivo conditions. Here a value of 260 dynes cm^{-2} was found on the inner walls of the renal bifurcation, which is only just below the lower limit of the acute yield stress measured by Fry (1968; 295 dynes cm^{-2}). Therefore, high shear stresses may indeed contribute to the occurrence of lesions in channels of certain geometry.

On the other hand, Caro et al., (1971) suggested that the

distribution of early atheroma in man is coincident with those regions in which arterial wall shear stress is relatively low, such as the walls of curved vessels and at the hips of bifurcations, while the development of lesions is inhibited in high shear stress regions. In contrast to the hypothesis that atheroma are associated with wall damage due to the motion of blood, it is proposed that their location is determined by a shear-dependent mass transport of lipids or lipoproteins across the wall which would tend to accumulate in areas of low wall shear rate. However, subsequent experiments on the transport of C^{14}-cholesterol between serum and vessel wall in a perfused segment of the artery failed to reveal any shear rate dependence of this process (Caro and Nerem, 1973).

(2) Hemostasis and Thrombosis

(a) Thrombosis and atherosclerosis. Hemostasis, a natural defence mechansism, was first observed as the participation of blood platelets by Bizzozero (1882), and Eberth and Schimmelbusch (1886). When a vessel is cut, platelets together with some leukocytes are found to adhere immediately to the site of injury where they form aggregates. As the aggregates grow in size, a fibrous network begins to appear at the periphery of the platelet mass to strengthen its structure and entrap numbers of red cells. In this way a hemostatic plug is formed, the size and life span of which are regulated under normal conditions to suit physiological needs by delicate control systems in the circulation. When this mechanism fails to work, as in hemophilia, a person bleeds uncontrollably because a hemostatic plug cannot form. On the other hand, if the hemostatic plug grows beyond physiological needs, it

will result in the vascular disease thrombosis.

The role of thrombosis, in initiating atherosclerosis was first proposed by Rokitansky (1884) and later revived by Duguid (1948, 1955), Mitchell and Schwartz (1963), and Osborn, (1963). It was suggested that since fibrin and platelets (Packham et al., 1967) have been found in atherosclerotic plaques, lesions may arise from thrombi deposited on the intimal surface and these would later be incorporated into the arterial wall by an overgrowth of the endothelium. The lipid content of the plaque would then be derived from the breakdown of leukocytes and platelets in the thrombi. While the latter part of this theory has not gained universal support (Walton, 1975), it is true that there is a striking similarity between the sites for deposition of platelet aggregates and the development of atheromatous plaques. Thus, the formation of platelet thrombi in vivo has been observed at sites downstream from bifurcations (Geissinger et al., 1962; Kwaan et al., 1967; Packham et al., 1967), sharp bends (Fox and Hugh, 1966), stenoses (Mitchell and Schwartz, 1963) and implanted rings in the vena cava (Gott et al., 1967). The deposition of platelet aggregates at similar locations in an in vitro system has been detected using extracorporeal shunts of collodion (Rowntree and Shionoya, 1927; Shionoya, 1927), plastic (Murphy et al., 1962; Mustard et al., 1962) and glass (Fry et al., 1965).

(b) Flow and thrombosis. From fluid mechanical considerations, it can be shown that bifurcations, T-joints, sharp bends, and constrictions, are places where flow is disturbed and where separation of the streamlines from the vessel wall and the formation of vortices can occur (Prandtl, 1952; Schlichting, 1960).

Therefore, many researchers cite fluid mechanical factors as a cause of atheroma and thrombus formation (Stehbens, 1959; Texon et al., 1960; Murphy et al., 1962; Mustard et al., 1962; Fox and Hugh, 1966; Gutstein and Schneck, 1967; Fry, 1968; Goldsmith, 1972; Rodkiewicz, 1975). Even in vitro studies of the formation of platelet thrombi on prosthetic devices have been linked to unfavorable vessel geometry causing flow separation with vortex formation (Fry et al., 1965; Blackshear et al., 1971; Smith et al., 1972; Stein and Sabbah, 1974; Benis et al., 1975).

This has led researchers in the field of Chemical, Biomedical and Mechanical Engineering to compute the flow patterns and distributions of fluid shear rates in pure Newtonian liquids flowing through simple models of two dimensional constrictions (Lee and Fung, 1970,1971), bifurcations (Hung and Naff, 1969; Hunt, 1969; Lynn et al., 1970; Schreck, 1972; Zamir and Roach, 1973; Friedman et al., 1975; O'Brien et al., 1976) and sudden expansions of lumen (Macagno and Hung, 1967; Hung, 1970). These studies, while giving useful information on the influence of steady and pulsatile flow on flow patterns and distributions of fluid shear stresses, still leave open the question of the effect of flow separation on the behavior of the suspended blood corpuscles particularly with respect to their interaction with each other and the vessel wall. The answer to this question is of vital importance since it is the blood cells which are the participants in thrombus formation.

It has been shown that the vortex is a region in which particles undergo large variations in shear rate (Yu and Goldsmith,

1973; Karino and Goldsmith, 1977a). Perhaps of greater significance to the in vivo situation is the relatively long times that blood cells spend in the vortex. Recent experiments in which suspensions of human platelets were subjected to flow through a model expansion have shown that their adhesion to the tube wall is greater in the annular vortex than elsewhere in the tubes (Karino and Goldsmith, 1977b). Furthermore, at the relatively lower shear rates observed in the vortex, collisions between platelets resulted in small aggregates which did not separate after collision. Instead, these remained within the vortex migrating into the center, while single red cells and platelets migrated outward into the mainstream (Goldsmith and Karino, 1977). In the presence of very small quantities of aggregating agents, such as ADP or thrombin, the platelet aggregates continued to grow in size until one large particle occupied a large portion of the annular vortex.

It was also shown that the region of separated flow is one of low hematocrit, thus decreasing the availability of oxygen for the arterial wall which may also lead to an increase in atherogenesis (Back, 1975a,b).

(3) Bifurcations

(a) Flow separation. There is considerable evidence that primary atherosclerotic lesions and platelet thrombi tend to form at bifurcations (Stehbens, 1960; Mitchell and Schwartz, 1965; Fox and Hugh, 1966; Hugh and Fox, 1970; Caro et al., 1971). Moreover, there is evidence from in vitro studies that pronounced secondary flow patterns, often resulting in flow separation, can

occur in models of *in vivo* bifurcations whose diameters exceed 1 cm (Caro *et al.*, 1971; Roach *et al.*, 1972; Brech and Bellhouse, 1973; Rodkiewicz and Roussel, 1973). These facts provided the rationale for the present work, which is concerned with the behavior of particles in such flows, especially in the regions of flow separation.

(b) Characteristics of bifurcations in the vasculature. The geometry of bifurcations is generally described in terms of the bifurcation angle θ, the area ratio α, defined as the sum of the cross-sectional area of the daughter branches to the cross-sectional area of the parent branch, and the radii of curvature of the outer walls, r_1 and r_2 (Figure 1).

Examination of the larger arterial bifurcations in man have revealed that α for the aortic bifurcation lies between 0.6 and 1.11 (Hess, 1927; Beales and Steiner, 1972; Caro *et al.*, 1971; Gosling *et al.*, 1971; Arnot and Louw, 1972; Lallemand *et al.*, 1972). The range of area ratios found was due to the differences in age and health of each subject as well as the location of the bifurcation used for each study (Stehbens, 1974; Gosling *et al.*, 1971). Gosling *et al.*, (1971), from a study of 50 aortograms on humans with no radiological evidence of atherosclerosis, showed that at birth the area ratio of the aortic bifurcation was 1.11 and that it progressively decreased until at 50 years of age the area ratio becomes about 0.75. Caro *et al.*, (1971) using aortograms and resin casts, and Beales and Steiner, (1972) using aortograms only on normal subjects of various ages 12-50, made measurements of the aortic bifurcation finding the area ratio to have a mean value of

Figure 1. Coordinates used to describe the geometry and dimensions of a Y-bifurcation. The origin of the axial coordinates x_o, x_1 and x_2 is taken as the plane in which the projection of the parent and daughter tube axes intersect.

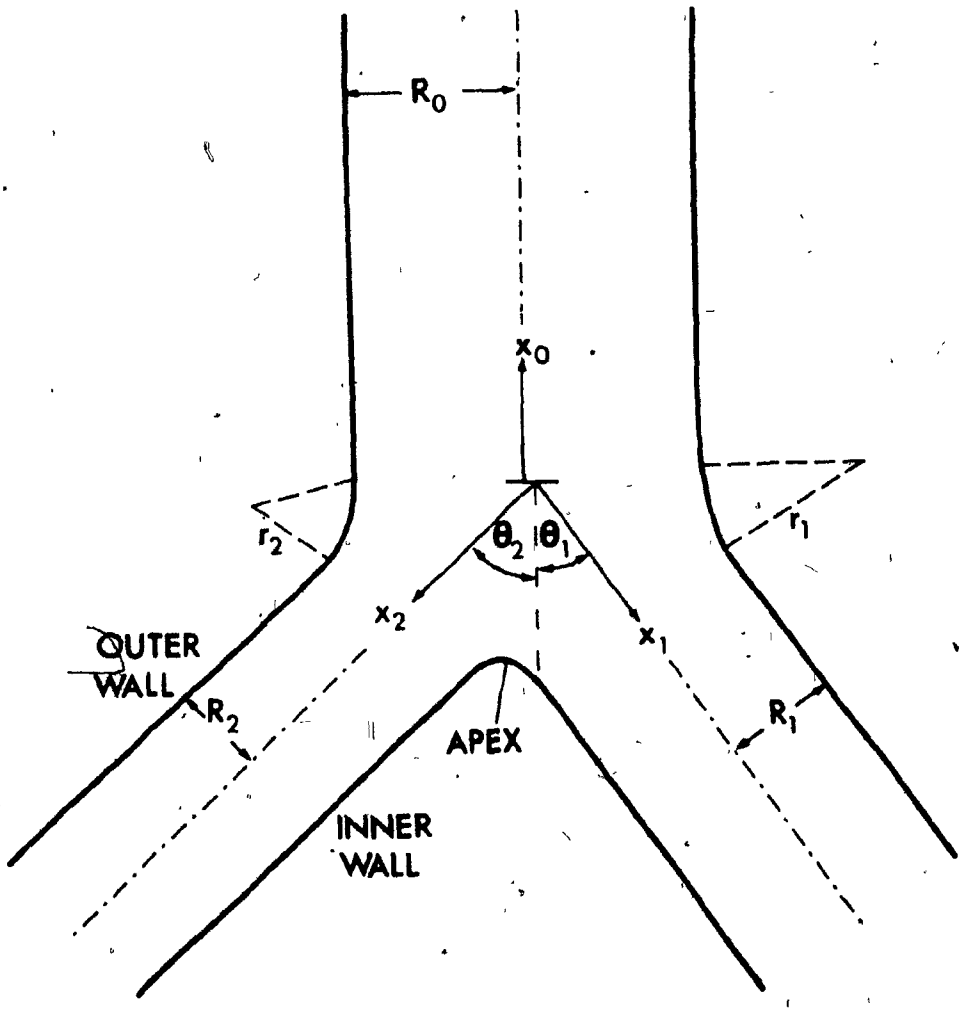
R_0
x_0
r_2
r_1
θ_2
θ_1
x_2
x_1
OUTER WALL
R_2
R_1
APEX
INNER WALL

0.75 and 0.77 respectively. They also found that in the large proximal arteries in man, the area ratios were between 0.8 and 1.2. Thoma (1896), making measurements of the lower human aorta, stated the area ratio was 1.0.

Gosling et al., (1971) also studied the area ratio of the aortic bifurcation in a dog and cockerel using aortograms. They found the area ratio of the dog ranged from 1.16 to 1.35 (mean value 1.23) and in the cockerel 1.05 to 1.28 (mean value 1.16). With a dietary induced atherosclerosis, Newman et al., (1971) found the area ratio in cockerels had decreased to a mean value of 0.86. They also showed that humans with radiographic evidence of atherosclerosis had a decrease in area ratios, larger than what would be expected of healthy humans at that age according to Gosling et al., (1971). Lallemand et al., (1972) suggested that because the area ratio in the abdominal aortic junction was low in 5 of 6 women operated on due to an aortic occlusion, this abnormality was associated with the initiation of atheroma of the lower aorta.

It should be noted, however, that the various methods of calibration using angiograms (Caro et al., 1971; Gosling, et al., 1971), the external diameter (Lallemand et al., 1972), the internal circumference (Arnot and Louw, 1972) do not measure the same cross-sectional area and except for the angiograms, do not deal with the arteries in vivo, and hence their validity has been questioned (Stehbens, 1974). Furthermore, unless measurements of vessel diameter were made at sites far from the apex of the bifurcation, considerable variations in α can be expected because of the rapidly changing cross-sectional areas at the entry of the daughter branches (Thoma, 1897; Stehbens, 1974).

It has been estimated that to minimize the pressure drop due to viscous dissipation of energy, the area ratio of a symmetric bifurcation with steady equal flow in the daughter branches should be 1.26 (Caro et al., 1971; Lighthill, 1972). This value was experimentally determined to be 1.33 (Hamilton, 1949). Womersley, (1958) has shown theoretically that in pulsatile flow reflection of the pressure pulse waves will vary with the area ratio. Gosling et al., (1971) extended Womersley's work and have shown that pressure pulse reflection is a minimum when the area ratio is 1.15. This value would only be matched at birth when the area ratio of the aortic junction is 1.11 ± 0.02.

(4) Scope of the Thesis

The present work is limited to an investigation of the behavior of neutrally buoyant rigid spheres of diameter < 35 μm in dilute suspensions flowing through small Y-bifurcations of various α and radii of curvature, and through T-bifurcations, both open and partially occluded. It forms part of a continuing series of investigations using microrheological techniques to study the flow of corpuscles through straight tubes (Goldsmith, 1971,1972; Frojmovic et al., 1976), obstructions (Yu and Goldsmith, 1973; Goldsmith et al., 1976), and sudden expansions (Karino and Goldsmith, 1977a). The aim of microrheology is to build up a knowledge of the overall or macroscopic flow properties of a suspension, piece by piece, from an investigation of the microscopic flow behavior of the individual suspended particles and surrounding elements of fluid (Goldsmith and Mason, 1967). Here in order to observe the motions

of the microscopic spheres, small but realistic bifurcations had to be built and this was initially achieved by using the vasculature of the dog mesentery.

As described in Chapter II, the results obtained revealed the existence of flow conditions such that platelet concentrations may increase at the hips of a bifurcation, conditions which may lead to the formation of thrombi and their deposition on the vessel walls.

REFERENCES

ANITSCHKOW, N. (1933). Experimental atherosclerosis in animals In "Atherosclerosis" (E.V. Cowdry, ed.), pp. 271-322, Macmillan, New York.

ARNOT, R.S., AND LOUW, J.H. (1972). Atheroma of the aortic bifurcation. Brit. Med. J. 3, 470-473.

ASCHAFF, L. (1924). Lectures in Pathology. pp. 131-135, Hoeber, New York.

BACK, L.H. (1975a). Theoretical investigation of mass transport to arterial walls in various blood flow regions. I. Flow field and lipoprotein transport. Mathematical Biosciences 27, 231-262.

BACK, L.H. (1975b). Theoretical investigation of mass transport to arterial walls in various blood flow regions. II. Oxygen transport and its relationship to lipoprotein accumulation. Mathematical Biosciences 27, 263-285.

BEALES, J.S.M., AND STEINER, R.E. (1972). Radiological assessment of arterial branching coefficients. Cardiovascular Res. 6, 181-186.

BENIS, A.M., NOSSEL, H.L., ALEDORT, L.M., KOFFSKY, R.M., STEVENSON, J.F., LEONARD, E.F., SHIANG, H., AND LITWAK, R.S. (1975). Extracorporeal model for study of factors affecting thrombus formation. Thromb. Diathes. Haemorrh. 34, 127-144.

BIZZOZERO, G. (1882). Ueber einen neuen Formbestandtheil des Blutes und dessen Rolle bei der Thrombose und der Blutgerinnung. Virchows Archiv. Path. Anat. 90, 261-332.

BLACKSHEAR, P.L., FORSTROM, R.J., LORBERBAUM, M., GOTT, V.L., AND SOVILJ, R. (1971). A role of flow separation and recirculation in thrombus formation on prosthetic surfaces. AIAA 9th Aerospace Sciences Meeting, Paper 71-103, New York, N.Y.

BRECH, R., AND BELLHOUSE, B.J. (1973). Flow in branching vessels. Cardiovascular Res. 7, 593-600.

CARO, C.G., FITZ-GERALD, J.M., AND SCHROTER, R.C. (1971). Arterial wall shear. Observation, correlation and proposal of a shear dependent mass transfer mechanism for atherogenesis. Proc. Roy. Soc. (London). B 177, 109-159.

CARO, C.G., AND NEREM, R.M. (1973). Transport of C^{14}-cholesterol between serum and wall in the perfused dog common carotid artery. Circ. Res. 32, 187-205.

DUGUID, J.B. (1926). Atheroma of the aorta. J. Path. Bact. 29, 371-387.

DUGUID, J.B. (1948). Thrombosis as a factor in the pathogenesis of aortic atherosclerosis. J. Path. Bact. 60, 57-61.

DUGUID, J.B. (1955). Mural thrombosis in arteries. Brit. Med. Bull. 11, 36-38.

EBERTH, C.J., AND SCHIMMELBUSCH, C. (1888). "Die Thrombose nach Versuchen und Leichenbefunden", p. 144, V. Enke, Stuttgart.

FEUERSTEIN, I.A., ELMASRY, O.A., AND ROUND, G.F. (1976). Arterial bifurcation flows — effects of flow rate and area ratio. Can. J. Physiol. Pharmacol. 54, 795-808.

FOX, J.A., AND HUGH, A.E. (1966). Localization of atheroma. A theory based on boundary layer separation. Brit. Heart J. 28, 388-399.

FOX, J.A., AND HUGH, A.E. (1970). Static zones in the internal cartoid artery: correlation with boundary layer separation and stasis in model flows. Brit. J. Radiol. 43, 370-376.

FRIEDMAN, M.H., O'BRIEN, V.O., AND EHRLICH, L.W. (1975). Calculations of pulsatile flow through a bifurcation. Circ. Res. 36 277-285.

FROJMOVIC, M.M., NEWTON, M., AND GOLDSMITH, H.L. (1976). The microrheology of mammalian platelets. Studies of rheo-optical transients and flow in tubes. Microvasc. Res. 11, 203-215.

FRY, D.L. (1968). Acute vascular endothelial changes associated with increased blood velocity gradients. Circ. Res. 22, 165-197.

FRY, D.L. (1969). Certain histological and chemical responses of the vascular interface to acutely induced mechanical stress in the aorta of the dog. Circ. Res. 24, 93-108.

FRY, F.J., EGGLETON, R.C., KELLY, E., AND FRY, W.J. (1965). Properties of the blood interface essential to successful artificial heart function. Trans. Amer. Soc. Artif. Int. Organs 11, 307-317.

GEISSINGER, H.D., MUSTARD, J.F., AND ROWSELL, H.C. (1962). The occurrence of microthrombi on the aortic endothelium of swine. Can. Med. Assn. J. 87, 405-408.

GESSNER, F.B. (1973). Hemodynamic theories of atherogenesis. Circ. Res. 33, 259-266.

GOLDSMITH, H.L. (1971). Red cell motions and wall interactions in tube flow. Fed. Proc. 30, 1578-1588.

GOLDSMITH, H.L. (1972). The flow of model particles and blood cells and its relation to thrombogenesis. In "Progress in hemostasis and thrombosis", Vol. 1. (T.H. Spaet, ed.), pp. 97-139, Grune & Stratton, New York.

GOLDSMITH, H.L., AND KARINO, T. (1977). Microscopic considerations: the motions of individual particles. N.Y. Acad. Sci. (In Press).

GOLDSMITH, H.L., MARLOW, J., AND YU, S.K. (1976). The effect of oscillatory flow on the release reaction and aggregation of human platelets. Microvasc. Res. 11, 335-359.

GOLDSMITH, H.L., AND MASON, S.G. (1967). The microrheology of dispersions. In "Rheology : Theory and Applications", Vol. IV (F.R. Eirich, ed.), pp. 85-250, Academic Press, New York.

GOSLING, R.G., NEWMAN, D.L., BOWDEN, N.L.R., AND TWINN, K.W. (1971). The area ratio of normal aortic junctions. Aortic configuration and pulse-wave reflection. Brit. J. Radiol. 44, 850-853.

GOTT, V.L., RAMOS, M.D., NAJJAR, F.B., ALLEN, J.L., AND BECKER, K.E. (1969). The in vivo screening of potential thrombo-resistant materials. In "Artificial Heart Program Conference" (R.J. Hegyeli, ed.), p. 181, Washington D.C., U.S. Govt. Printing Office.

GUTSTEIN, W.H., AND SCHNECK, D.J. (1967). In vitro boundary layer studies of blood flow in branched tubes. J. Atheroscler. Res. 7, 295-299.

HAMILTON, W.F. (1949). Regulation of arterial pressure. In "A Textbook of Physiology" (J.F. Fulton, ed.), 16th Ed., pp. 751, W.B. Saunders Co., Philadelphia, Pa.

HESS, W.R. (1927). Handbuch der normalen und pathologischen Physiologie, Bd. VII, Teil 2, pp. 804-933, Bethe, Berlin.

HUNG, A.E., AND FOX, J.A. (1970). The precise localization of atheroma and its association with stasis at the origin of the internal carotid artery - a radiographic investigation. Brit. J. Radiol. 43, 377-383.

HUNG, T.-K. (1970). Vortices in pulsatile flows. In "Proc. Fifth Intern. Congr. Rheology", Vol. 2 (S. Onogi, ed.), pp. 115-127. Univ. of Tokyo Press and Univ. Park Press.

HUGH, T.-K., AND NAFF, S.A. (1969). A mathematical model of systolic blood flow through a bifurcation. Proc. 8th Intern. Conf. Med. Biol. Engr. Paper no. 20-11.

HUNT, W.A. (1969). Calculation of pulsatile flow across bifurcations in distensible tubes. Biophysical J. 9, 993-1005.

KARINO, T., AND GOLDSMITH, H.L. (1977a). Flow behavior of blood cells and rigid spheres in an annular vortex. Phil. Trans. Roy. Soc. (London). (In Press).

KARINO, T., AND GOLDSMITH, H.L. (1977b). Platelet adhesion to collagen-coated walls in an annular vortex. Forthcoming publications.

KWAAN, H.C., HARDING, F., AND ASTRUP, T. (1967). Platelet behavior in small blood vessels in vivo. In "Platelets: their role in Hemostasis and Thrombosis" (Brinkhous et al., eds.), pp. 208-220. Thromb. Diathes. Haemorrh. Suppl 26. Schattauer, Stuttgart.

LALLEMAND, R.C., BROWN, K.G.E., AND BOULTER, P.S. (1972). Vessel dimensions in premature atheromatous disease of aortic bifurcation. Brit. Med. J. 2, 255-257.

LEE, J.-S., AND FUNG, Y.-C. (1970). Flow in locally constricted tubes at low Reynolds numbers. J. Appl. Mech. 37, 9-16.

LEE, J.-S., AND FUNG, Y.C. (1971). Flow in non-uniform small blood vessels. Microvasc. Res. 3, 272-287.

LIGHTHILL, M.J. (1972). Physiological fluid dynamics. J. Fluid Mech. 52, 475-497.

LING, S.C., ATABECK, H.B., FRY, D.L., PATEL, D.J., AND JANICKI, J.S. (1968). Application of heated-film velocity and shear probes to hemodynamic studies. Circ. Res. 23, 789-801.

LING, S.C., ATABEK, H.B., AND CARMODY, J.J. (1969). Pulsatile flow in arteries. In "Proc. 12th Interm. Congr. Appl. Mech." (M. Hetenyi and W.E. Vincenti, eds.), pp. 277-291, Springer-Verlag. Berlin.

LYNN, N.S., FOX, V.G., AND ROSS, L.W. (1970). Flow patterns at arterial bifurcations. In "Symposium on Recent Developments in Biological Fluid Mechanics" Paper 59d. Amer. Inst. Chem. Eng., New York.

MACAGNO, E.O., AND HUNG, T.-K. (1967). Computational and experimental study of a captive annular eddy. J. Fluid Mech. 28, 43-64.

MITCHELL, J.R.A., AND SCHWARTZ, C.J. (1963). The relationship between myocardial lesions and coronary artery disease. II. A selected group of patients with massive cardiac necrosis or scarring. Brit. Heart J. 25, 1-24.

MITCHELL, J.R.A., AND SCHWARTZ, C.J. (1965). "Arterial Disease", Blackwell, Oxford.

MURPHY, E.A., ROWSELL, H.C., DOWNIE, H.G., ROBINSON, G.A., AND MUSTARD, J.F. (1962). Encrustations and atherosclerosis: the analogy between early lesions and deposits in extracorporeal circulation. Canad. Med. Assn. J. 87, 259-274.

MUSTARD, J.F., MURPHY, E.A., ROWSELL, H.C., AND DOWNIE, H.G. (1962). Factors influencing thrombosis formation in vivo. Amer. J. Med. 33, 621-647.

NEWMAN, D.L., GOSLING, R.G., AND BOWDEN, N.L.R. (1971). Changes in aortic distensibility and area ratio with the development of atherosclerosis. Atherosclerosis 14, 231-240.

O'BRIEN, V.O., EHRLICH, L.W., AND FRIEDMAN, M.H. (1976). Unsteady flow in a branch. J. Fluid Mech. 75, 315-336.

OSBORN, G.R. (1963). "The Incubation Period of Coronary Thrombosis", Butterworth, London.

PACKHAM, M.A., ROWSELL, H.C., JØRGENSEN, L., AND MUSTARD, J.F. (1967). Localized protein accumulation in the wall of the aorta. Exptl. Molec. Path. 7, 214-232.

PRANDTL, L. (1952). "Essentials of Fluid Dynamics", pp. 135-141, Blackie and Son Ltd., London & Glasgow.

ROACH, M.R., SCOTT, S., AND FERGUSON, G.G. (1972). The hemodynamic importance of the geometry of bifurcations in the circle of Willis (glass model studies). Stroke 3, 255-267.

RODKIEWICZ, C.M. (1975). Localization of early atherosclerotic lesions in the aortic arch in the light of fluid flow. J. Biomech. 8, 149-156.

RODKIEWICZ, C.M., AND ROUSSEL, C.L. (1973). Fluid mechanics in a large arterial bifurcation. Trans. ASME, 108-112.

ROKITANSKY, C. (1844). "A Manual of Pathological Anatomy" (Translated, G.E. Day, 1852), Vol. 4, pp. 261-272. Sydenham Society, London.

ROWNTREE, L.G., AND SHIONOYA, T. (1927). Studies in experimental extracorporeal thrombus formation. Method for direct observation of extracorporeal thrombus formation. J. Exp. Med. 46, 7-18.

SCHLICHTING, H. (1960). "Boundary Layer Theory", pp. 24-43, McGraw Hill, New York.

SCHRECK, R.M. (1972). Laminar flow through bifurcations with applications to the human lung. Ph.D. Thesis, Northwestern Univ., Evanston, Ill.

SCHWARTZ, C.J., ARDLIE, N.G., CARTER, R.F., AND PATERSON, J.C. (1967). Gross aortic sudanophilia and hemosiderin deposition. A study on infants, children, and young adults. Arch. Path. 83, 325-332.

SHIONOYA, T. (1927). Studies in experimental extracorporeal thrombosis. III. Effects of certain anticoagulants (heparin and hirudin) on extracorporeal thrombosis and on the mechanism of thrombus formation. J. Exp. Med. 46, 19-26.

SMITH, R.L., BLICK, E.F., COALSON, J., AND STEIN, P.D. (1972). Thrombus production by turbulence. J. Appl. Physiol. 32, 261-264.

STEHBENS, W.E. (1959). Turbulence of blood flow. Quart. J. Exp. Physiol. 44, 110-117.

STEHBENS, W.E. (1960). Focal intimal proliferations in the cerebral arteries. Amer. J. Path. 36, 289-301.

STEHBENS, W.E. (1974). Changes in the cross-sectional area of the arterial fork. Angiology 25, 561-575.

STEIN, P.D., AND SABBAH, H.N. (1974). Measured turbulence and its effect on thrombus formation. Circ. Res. 35, 608-614.

STRONG, J.B., AND McGILL, H.C., Jr. (1962). The natural history of coronary atherosclerosis. Amer. J. Path. 40, 37-49.

TEXON, M., IMPARATO, A.M., AND LORD, J.W., Jr. (1960). The hemodynamic concept of atherosclerosis: The experimental production of hemodynamic arterial disease. Arch. Surg. 80, 47-53.

THOMA, R. (1896). Textbook of General Pathology (A. Bruce, trans.), Vol. I, pp. 273-275, Adam and Charles Black, London.

VIRCHOW, R. VON (1862). Phlogose und Thrombose im Gefässystem. Gesammelte Abhandlungen zur Wissenschaftlichen Medizin. Max Hirsch, Berlin.

WALTON, K.W. (1975). Pathogenetic mechanisms in atherosclerosis. Amer. J. Cardiology 35, 542-558.

WESOLOWSKI, S.A., FRIES, C.C., SABINI, A.M., AND SAWYER, P.N. (1962). Significance of turbulence in hemic systems and in the distribution of the atherosclerotic lesion. Surgery 57, 155-162.

WESOLOWSKI, S.A., FRIES, C.C., SABINI, A.M., AND SAWYER, P.N. (1965). Turbulence, intimal injury, and atherosclerosis. In "Biophysical Mechanisms in Vascular Homeostasis and Intravascular Thrombosis" (P.N. Sawyer, ed.), pp. 147-157. Appleton Crofts, New York.

WILLIS, G.C. (1954). Localizing factors in atherosclerosis. Canad. Med. Assn. J. 70, 1-8.

WOMERSLEY, J.R. (1958). Oscillatory flow in arteries II: The reflection of the pulse wave at junctions and rigid inserts in the arterial system. Physics in Med. Biol. 2, 313.

YU, S.K., AND GOLDSMITH, H.L. (1973). Behavior of model particles and blood cells at spherical obstructions in tube flow. Microvasc. Res. 6, 5-31.

ZAMIR, M., AND ROACH, M.R. (1973). Blood flow downstream of a two-dimensional bifurcation. J. Theor. Biol. 42, 33-48.

CHAPTER II

Particle behavior in flow through small bifurcations

ABSTRACT

The effects of branching vessels on circulating blood cells were modeled using dilute suspensions of rigid spheres $\leq$ 35 μm diameter flowing through dissected, fixed and mounted dog mesentery bifurcations, and through model Y- and T-bifurcations having tube diameters < 1 mm. Particle paths were observed and photographed by taking 16 mm cine films through a low power microscope.

Only a moderate secondary flow, and no separation of streamlines was found in the dog mesentery bifurcation (area ratio = 1.5), even at Reynolds numbers Re of 150. In the model Y-bifurcations having much smaller radii of curvature on the outer walls, and higher area ratios ($\geq$ 2.0), a pronounced secondary crossflow and flow separation at Re > 80 was observed at the entry of the daughter branches. Particles moved laterally across the streamlines of the primary flow and entered spiral, triangular shaped vortices at the outer wall of the hips of the bifurcation.

Flow in a symmetric T-bifurcation was also studied. No flow separation was observed, even at Re = 205, unless one of the daughter branches was partially occluded when a spiral vortex formed at the entry of the obstructed branch. The formation and growth of this vortex was determined as a function of the ratio of flow rates in the daughter branches (degree of occlusion) and, at a given degree of occlusion, as a function of the parent tube Re.

The distribution of rigid spheres in the vortices of the Y- and T-bifurcations were found to depend on particle diameter.

The larger spheres were absent from streamlines originating very close to the tube walls, due to the exclusion of particle centers within one sphere radius of the wall, as well as inward radial migration.

LIST OF SYMBOLS

n_D	refractive index
Q_o, Q_1, Q_2	volume flow rates in the parent, right and left branches of the bifurcation, respectively
r_1, r_2	respective radii of curvature of right and left outer walls of the bifurcation
R	radial distance from the tube axis
R_o, R_1, R_2	tube radius of the parent, right and left branches of the bifuraction
ΔR	projection in the median plane of the width of vortex in the partially occluded branch of a T-bifurcation
Re	tube Reynolds number = $2R_o\bar{U}_o\rho/\eta$
$\bar{t}$	$\Delta R/\bar{U}_o$
$u_o(R)$; $u_o(0)$	particle translational velocity at radial distance R in tube flow; value at the tube axis
$\bar{U}_o$	mean linear fluid velocity in parent tube = $Q_o/\pi R_o^2$
x_o, x_1, x_2	distances in the axial direction in the parent, right and left branches of bifurcation, respectively
x_{2M}	maximum value of x_2 at the outermost orbit of vortex in the T-bifurcation
x_{2S}	value of x_2 at the separation point in the T-bifurcation

α	area ratio = $\pi(R_1^2 + R_2^2)/\pi R_o^2$
η	fluid viscosity
ρ; $\Delta\rho$	fluid density; particle − fluid density difference
τ	measured residence time of particles in the vortex
θ; θ_1, θ_2	bifurcation angle; bisector angles of right and left branches respectively

INTRODUCTION

This work is concerned with the behavior of particles suspended in liquids flowing through bifurcations resembling those found in the mammalian vasculature. It forms part of a continuing series of investigations in this laboratory designed to discover the effects of areas of disturbed flow and vortices on suspended blood cells (Yu and Goldsmith, 1973; Karino and Goldsmith, 1977). The studies are motivated by the fact that there is considerable evidence that primary atherosclerotic lesions and platelet thrombi tend to form at precisely those sites in the arterial tree where flow separation is likely to exist, e.g., constrictions or stenoses, and bifurcations (Geissinger et al., 1962; Mitchell and Schwartz, 1965; Spain, 1966; Kwaan et al., 1967; Fox and Hugh, 1970; Hugh and Fox, 1970; Caro et al., 1971). Indeed, it has long been suspected that fluid mechanical factors play an important role in the formation of thrombi (Stehbens, 1959; Texon et al., 1960; Fox and Hugh, 1966; Gutstein and Schneck, 1967; Fry, 1968; Goldsmith, 1972; Smith et al., 1972). This has led to a number of theoretical studies of the flow patterns and fluid stresses in Newtonian liquids moving through two-dimensional constrictions (Lee and Fung, 1971), bifurcations (Hung and Naff, 1969; Lynn et al., 1970; Schreck, 1972; Zamir and Roach, 1973; Friedman et al., 1975) and sudden expansions of lumen (Macagno and Hung, 1967; Hung, 1970). These have shown under what conditions of steady or pulsatile flow, regions of flow separation,

of high or low shear stress may occur. However, the effects of such flow regimes on the blood cells, the actual participants in thrombus formation, remained a matter of conjecture. Hence, as in the previous studies, the present work focusses on the movements of the individual suspended particles with particular emphasis on their behavior in regions of flow separation. To this end, bifurcations of small dimensions with channels of ~ 1 mm diameter were used and suspensions containing particles $\leq$ 35 μm diameter observed under a microscope. This involved the use of micro-rheological techniques previously described in studies of flow through straight tubes, as well as past obstructions and at sudden expansions of lumen (Goldsmith and Mason, 1975).

It was also desirable that certain features of the bifurcation such as the bifurcation angle θ, the radii of curvature r_1 and r_2 (Figure 1) and the area ratio α, defined as the ratio of the sum of the cross-sectional area of daughter branches to that of the parent branch, be typical of those found in the mammalian vasculature. Most published data on area ratios deal with measurements of the aortic and other proximal, major branches in the arterial tree (Hess, 1927; Caro et al., 1971; Arnot and Louw, 1972; Beales and Steiner, 1972). In man, the aortic bifurcation has $\alpha < 1$, although, Gosling et al. (1971) report that at birth $\alpha = 1.11$, thereafter decreasing with increasing age. In the dog and the cockerel (Gosling et al., 1971), as well as in the rabbit (Stehbens, 1974), $\alpha > 1$ in the aortic bifurcation. In man, for the more distal bifurcations, α increases to a value close to 1.0. As might be

Figure 1. Coordinates used to describe the geometry and dimensions of a Y-bifurcation. The origin of the axial coordinates x_o, x_1 and x_2 is taken as the plane in which the projections of the parent and daughter tube axes intersect.

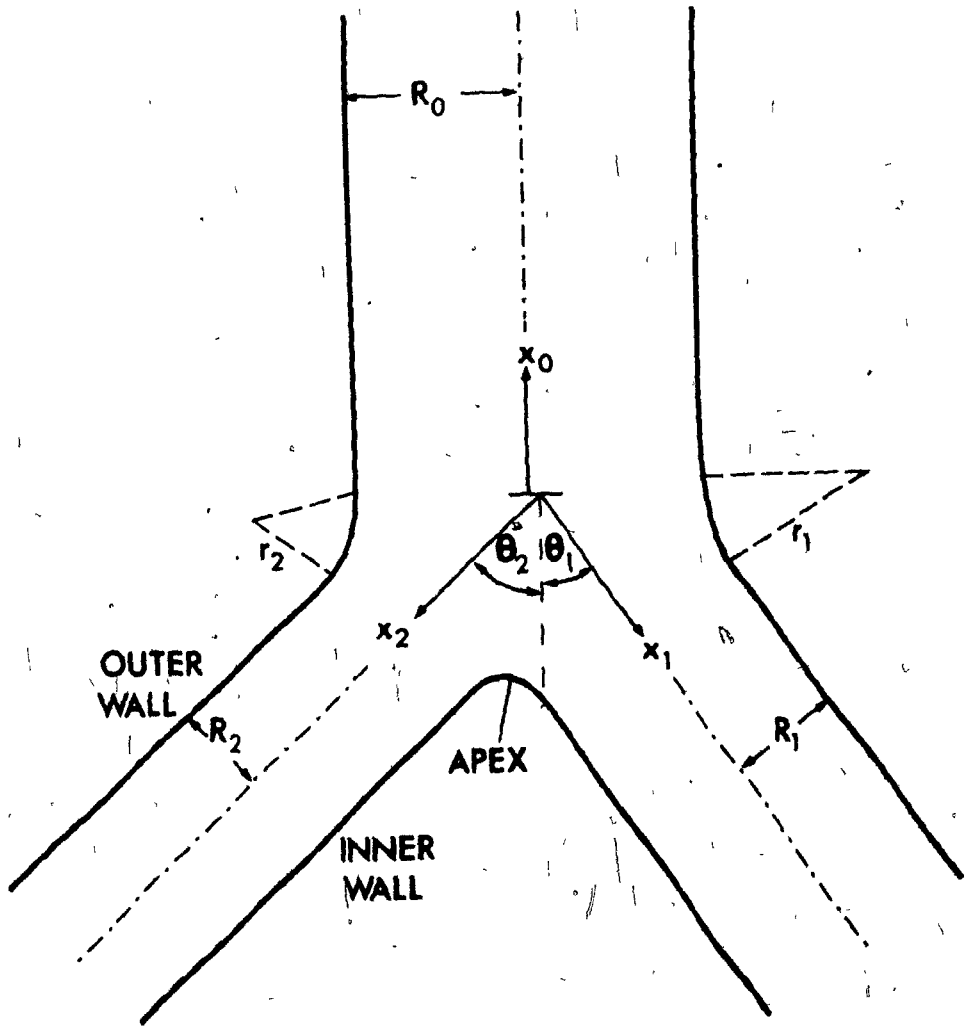
R_0
x_0
r_2
θ_2
θ_1
r_1
x_2
x_1
OUTER WALL
R_2
APEX
R_1
INNER WALL

expected, in persons with atherosclerotic disease, α in the aortic bifurcation decreases (Lallemand et al., 1972) from the values found in healthy individuals. When one daughter branch becomes appreciably or totally occluded one would expect considerable disturbance to the normal flow patterns, perhaps resulting in an area of flow separation at the entry of the occluded branch (Kreid et al., 1974).

As regards the bifurcation angles, these appear to vary widely, perhaps covering a range from 30° to 120°, and the radii of curvature are generally appreciably larger than the diameters of the parent vessel (e.g. hollow vascular replica of rabbit ear; Meiselman and Cokelet, 1975). The bends in the bifurcation are therefore gentle, and this is of some importance since the appearance of a secondary crossflow eventually resulting in flow separation is more likely to occur distal to sharp bends, other factors being equal. Here, due to a transverse pressure gradient, the elements of fluid with the highest kinetic energy move outside the bend while fluid with low kinetic energy near the walls will move to the inside giving rise to a secondary crossflow. Such flows have been observed in models of lung airway bifurcations (Schroter and Sudlow, 1969; Schreck, 1972) where the effects of differences in the radii of curvature on flow separation have been noted, as well as in models of large arterial bifurcations (Caro et al., 1971; Roach et al., 1972; Brech and Bellhouse, 1973; Rodkiewicz and Roussel, 1973; Feuerstein et al., 1976).

The present work represents an initial study of particle behavior in a bifurcation in which the paths of small rigid spheres

in dilute suspensions were analysed in detail over a range of Reynolds numbers. Initially, dog mesentery was chosen to obtain bifurcations typical of the vasculature. However, because of the high radii of curvature, flow separation was not observed even at the highest Reynolds numbers. Recourse was therefore had to models in which a combination of smaller radii of curvature and greater area ratios led to the appearance of regions of flow separation and spiral vortices at the hips of the bifurcation. Finally, particle behavior in flow through a 180° (T-) bifurcation and the effects of partially occluding one branch are described.

EXPERIMENTAL PART

(1) Dog Mesentery Bifurcations

After experimenting with several tissues in various animals, the vessels of the dog mesentery were considered the most suitable with respect to size, mounting and embedding. The arteries were approx. 1 mm in diameter, initially quite translucent and after fixation with aldehyde became transparent and durable. The bifurcation angles θ varied between 30° and 80° with mean area ratios $\bar{\alpha} = 1.22$ (Gosling et al., 1971). By comparison the vessels of the rabbit mesentery were subject to tear and collapse during dissection and the apex of one bifurcation was very close to that of the next. In the pig mesentery, there were very few bifurcations since most of the vessels exhibited triple and higher order branching.

(a) Preparation of the vessels. Mongrel dogs weighing between 20 and 30 kg were heparinized and sacrificed by intravenous

administration of an overdose of nembutal. The mesenteric artery was immediately cannulated and the mesentery excised while perfusing with an 0.9% saline solution at a pressure of 100 mm Hg. After flushing out the remaining blood, the vessels were fixed by washing with 200 ml of a solution of 4% formaldehyde and 1% gluteraldehyde in 200 mOsm phosphate buffer (McDowell and Trump, 1975).

A section of cannulated mesentery including the desired bifurcation was then mounted on a silicone rubber board and the tissue dehydrated by perfusing first with ethanol for one hour, followed by 15 min perfusions with ethanol-acetone mixtures of progressively increasing acetone content. The bifurcation was now laid on a glass microscope slide and the surrounding tissue and membranes dissected out to expose the arteries.

(b) Embedding of the bifurcation. To clear the tissue, the vessels were perfused with, and covered by, a solution of equal parts of acetone and Epon Resin 812 followed by pure epon resin after one hour. While still filled with epon, the bifurcation and polythene cannulating tubes were embedded on the glass slide in a 2 to 3 mm thick layer of epon medium consisting of 46% epon resin 812, 28% Dodecenyl-succinic Anhydride and 26% Nadic Methyl Anhydride containing 2% 2, 4, 6 Tridimethyl amino Methyl Phenol to catalyse the polymerization which proceeded in a 65°C oven for 8 hours. The resulting mounts were translucent and the motion of suspended particles in the vessel could be clearly seen under the microscope.

(2) Model Bifurcations

Flow channels having Y- and T-geometry were constructed by carefully drilling through polished blocks of epon, polymerized by

the above described method. The T-bifurcations were of uniform bore, with an internal diameter of 0.717 mm. The Y-bifurcations were symmetric with $\theta = 60°$, parent and daughter branches having approximately the same diameter. Channels of 0.83 and 1.10 mm were constructed. The walls of the Y-bifurcations exhibited some roughness: variations as high as ± 15 μm in the diameter over axial distances of 50 μm were observed.

The bifurcations were connected to the infusion syringe and the outflow reservoirs by 0.86 mm (I.D.) polythene tubing at distances of 20 mm, i.e. from 16 to 21 tube diameters, from the apex. This ensured the existence of fully developed velocity distributions at distances > 15 mm from the apex, even at the highest tube Reynolds numbers which prevailed in the experiments.

(3) Apparatus

Particle paths and velocities in flow through the bifurcations were obtained by analysis of 16 mm cine films taken through a horizontally positioned Reichert RC microscope with the microscope slide or epon block clamped on a vertically mounted, mechanically moveable platform, previously described (Goldsmith and Marlow, 1972). Details are given in Appendix A. Volume flow rates $Q_o < 0.1$ ml sec^{-1} were achieved with an infusion-withdrawal pump attached to the platform which drove the plunger of a 5 or 10 ml syringe. A Harvard 900 syringe infusion pump was used for higher Q_o. The platform could be driven in the vertical direction at speeds up to 10 mm sec^{-1} by means of a variable d.c. motor drive, and manually moved in the horizontal direction. This permitted tracking of the

particles only at very low Q_o (Re << 1); in the experiments described below, the films were taken with the platform and flow chamber stationary.

The suspensions were photographed at nominal magnifications from 15 to 60× with tungsten or mercury arc illumination provided by a Reichert Binolux twin lamp assembly. At mean linear flow rates $\bar{U}_o$ < 40 mm sec^{-1}, a Locam pin registered camera with a 1:9 rotating shutter (Red Lake Labs, Santa Clara, CA) was operated at speeds of 200 to 500 frames sec^{-1}. At higher $\bar{U}_o$, a Hycam camera (Red Lake Labs) with a 1:10 shutter was employed at framing speeds of 1,000 to 6,000 sec^{-1}. Plux X or Double X negative film was used, depending on the available illumination. A timing light generator produced electrical pulses at known intervals and triggered a neon glow lamp which put a timing mark onto the film.

The develped cine films were projected onto a drafting table and analysed frame by frame with the aid of a Kodak Analyst Stop-motion projector (LW International, Woodland Hills, CA).

(4) Suspensions

Dilute suspensions containing < 1% by volume of 15 and 32 μm diameter polystyrene spheres (Particle Information Services, Grants Pass, OR) in benzyl alcohol were used in most of the experiments. This system had the advantage of being almost neutrally buoyant ($\Delta\rho$ = 0.007 gm ml^{-1}) and, more important, of having the refractive indices of the alcohol (n_D = 1.540) very close to that of the polymerized epon (n_D = 1.536). This eliminated optical distortion due to refraction of light rays at the solid-liquid interface (Goldsmith and Mason, 1975) and the necessity of applying corrections

to the measured radial positions of the particles. The disadvantage of the system lay in the relatively poor contrast between the spheres (n_D = 1.510) and the benzyl alcohol. This necessitated the use of suspensions of high contrast 15 and 35 μm carbon microspheres ($\Delta\rho$ = 0.29, 3M Co., St. Paul, MN) in benzyl alcohol at the higher flow rates when the resolution on the cine films taken at > 3,000 frames sec^{-1} was poorer. The sedimentation rate of the 35 μm spheres, 35 μm sec^{-1}, although appreciable, was still < 1% of the mean linear fluid velocities in these runs.

The density of the benzyl alcohol (1.043 gm ml^{-1}) was determined using a pycnometer; its viscosity (0.057P at 23°C) was measured in a Cannon-Ubbelohde capillary viscometer.

All experiments were carried out in a room thermostated at 23°C ± 1°C.

RESULTS

(1) Dog Mesentery Bifurcations

(a) Morphology. A number of bifurcations from dog mesentery were mounted and studies made of the vessel dimensions and their geometry. Measurements of the tube diameters in the median plane were made under a low power microscope using a micrometer eyepiece. The tubes were filled with benzyl alcohol to avoid optical distortion. The radii of curvature r_1 and r_2 of the outer walls and the bisector angles θ_1 and θ_2 (Figure 1) were obtained by taking 35 mm photographs of the bifurcations through the microscope and projecting the negatives onto a drafting table. The results of the measurements

TABLE 1

DIMENSIONS AND GEOMETRY OF BIFURCATIONS FROM DOG MESENTERY[a)]

Diameters[b)]			Area Ratio	Angle			Radius of Curvature	
$2R_o$	$2R_1$	$2R_2$	α	θ_1	θ_2	$\theta_1 + \theta_2$	r_1	r_2
mm				degrees			mm	
1.09	0.89	0.75	1.13	30	34	64	1.62	3.84
0.86[c)]	0.71	0.63	1.24	22	18	40	7.25	8.31
0.94	0.83	0.69	1.32	17	20	37	5.07	10.86
0.84	0.51	0.71	1.09	33	21	54	5.16	2.39
0.95	0.83	0.62	1.19	31	33	64	3.52	3.02
1.18	0.89	0.72	0.95	33	30	63	–	–
1.06	0.81	0.89	1.27	36	41	77	3.94	3.09
1.12	1.13	1.02	1.83	30	31	61	–	–
1.29	0.71	0.95	0.84	35	33	68	2.18	2.29
1.50	1.00	1.02	0.92	27	22	49	3.52	3.79
1.32	1.04	1.01	1.20	28	27	55	–	–
1.06	0.70	0.84	1.06	30	31	61	2.16	2.05
0.96	0.76	0.69	1.13	36	35	71	1.64	2.05
0.99	0.73	0.93	1.43	32	34	66	3.05	3.25
0.88	0.81	0.78	1.62	28	27	55	2.96	2.30
1.17	0.95	0.81	1.13	40	40	80	1.49	1.63
0.92	0.43	0.83	1.02	22	18	40	19.8	3.97
0.98[c)]	0.89	0.83	1.55	33	30	63	1.72	2.11
Mean Values 1.06 ± 0.18	0.80 ± 0.17	0.82 ± 0.13	1.22 ± 0.26	–	–	59 ± 12	–	–

a) Coordinates are defined in Figure 1

b) Mean of 5 measurements made at 2 mm intervals from the junction

c) Bifurcations used in flow experiments.

are given in Table 1 for 18 bifurcations of which two were used for flow studies.

The values of the area ratio $\alpha = \pi(R_1^2 + R_2^2)/\pi R_o^2$ shown in the Table were calculated from mean values of 5 measurements of the radii made at equal intervals over 10 tube diameters upstream and downstream of the junction in each of the tubes. It should be noted that these are not necessarily the true area ratios since the calculation assumes circular cross-section. In fact, examination of thin serial sections cut in a plane normal to that of the bifurcation under the microscope revealed that, at distances > 2 diameters from the apex, the cross-section was often ellipsoidal although the major and minor diameters differed by no more than 10%. Closer to the apex, the cross-section became ovoid, then dumb-bell shaped just before the division of the channel (Stehbens, 1974). Immediately distal to the apex, the diameters of the daughter tubes decreased slightly, thereafter remaining approximately constant. The calculated α varied from 0.84 to 1.83, with most values in the range 1.0 to 1.3. The mean $\alpha = 1.22$ is close to the value given by Gosling *et al.*, (1971) for the much larger aortic bifurcation in the dog.

Most striking was the asymmetry of most of the bifurcations and the large radii of curvature of the outer walls, the latter being at least 30% greater and often 2 to 5× greater than the mean parent tube diameter. There were significant differences between the diameters of the daughter branches, usually >10% and in some cases >25%. The bifurcation angle varied from 37° to 80° with a mean value of 59°. The bisector angles were equal, or nearly equal in 6 cases, the other 12 exhibited differences from 2° to 12°.

(b) Flow in dog mesentery bifurcations. The flow of dilute suspensions consisting of mixtures of 15 and 32 μm diameter polystyrene spheres or of 15 and 35 μm carbon microspheres in benzyl alcohol, was observed in two of the mounted animal bifurcations whose geometry and dimensions are given in Table 1. Particle paths were traced from cine films over a range of flow rates, corresponding to parent tube Reynolds numbers

$$Re = \frac{2R_o\bar{U}_o\rho}{\eta}$$

from <1 to 150 ($\bar{U}_o$ and R_o are the mean velocity in, and radius of the parent tube, ρ and η being the respective density and viscosity of the benzyl alcohol). It was found that even at the highest Re obtained using 50 ml infusion syringes, when centerline particle velocities were of the order of 1.7 m sec^{-1}, no flow separation was observed in the bifurcations.

(i) Flow patterns. Particle paths measured in the median plane of the more symmetric bifurcation ($2R_o$ = 0.98 mm, α = 1.55) are illustrated in Figure 2. At relatively low flow rates, Re = 2.15 and $\bar{U}_o$ = 12.0 mm sec^{-1} (Figure 2a), the streamlines were parallel to the parent tube walls, but due to the asymmetry of the bifurcation (the right hand branch having a somewhat larger diameter than the left and receiving 52% of the total flow) they divided asymmetrically about the parent tube axis. Thus, particles on paths just to the right of the axis flowed into the smaller left hand daughter branch. On entering the daughter tubes, the streamlines again became parallel to the vessel walls.

Figure 2. The paths of 15 and 35 μm diameter carbon microspheres in benzyl alcohol flowing through a bifurcation from the dog mesentery; R_o = 0.49 mm, R_1 = 0.45 mm, R_2 = 0.41 mm. (a): $\bar{U}_o$ = 12.0 mm sec^{-1}, Re = 2.15; particle paths divide to the right of the parent tube axis. (b): $\bar{U}_o$ = 750 mm sec^{-1}, Re = 133; particle paths now divide symmetrically about the tube axis and secondary flow appears, as shown by the dashed lines. The numbers in the diagram refer to particle velocities, in mm sec^{-1}, at the positions indicated.

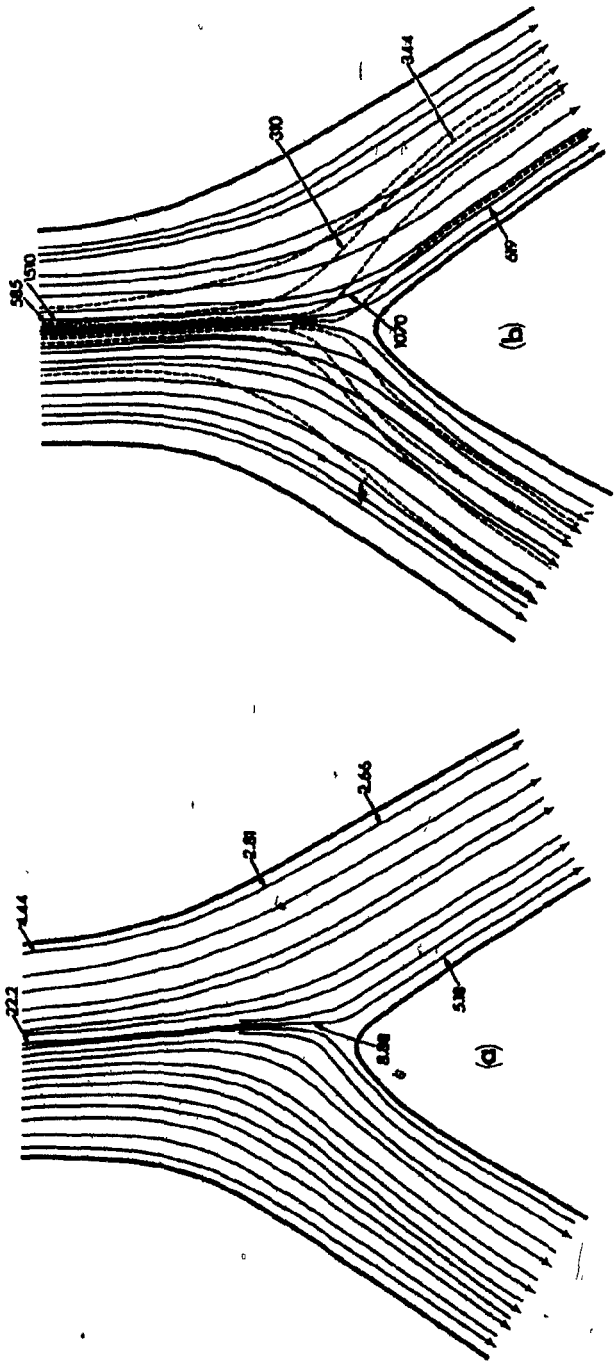
3.44
3.30
5.85
5.50
10.50
(b)
2.66
2.88
4.44
2.22
5.38
8.88
(a)

At higher Re, there was a noticeable shift in the streamlines towards the left branch. This is illustrated in Figure 2b at Re = 133 ($\bar{U}_o$ = 750 mm sec^{-1}) where the streamlines are seen to divide symmetrically about the parent tube axis. More significant is the appearance of secondary flow patterns at these Reynolds numbers, as shown by the dashed streamlines in the Figure. Particles travelling on such paths were located above or below the median plane normal to the viewing axis, but were visible because of the appreciable depth of focus (from ±70 to ±100 μm) existing at the low magnifications used in these experiments (from 15 to 50×). Such particles were recognized by their velocities, which were lower than those of spheres in the mainstream at the same apparent radial distance but flowing in the median plane (e.g. the spheres entering the bifurcation on the 9th and 10th streamlines drawn in Figure 2b have velocities of 1,510 and 585 mm sec^{-1} respectively).

The secondary flow patterns were such that spheres at apparent radial positions close to the parent tube axis travelled along streamlines which crossed the primary flow in the junction near the apex and moved out towards the outer walls of the daughter tubes before resuming flow in the axial direction. No differences in flow behavior between 15 and 35 μm spheres could be detected.

As will become evident later, in bifurcations having smaller radii of curvature, at sufficiently high Re these secondary flow patterns develop into vortices at the outer walls of the daughter branches (Schreck, 1972; Brech and Bellhouse, 1973).

(ii) Velocity distributions and shear rates. All spheres, both in the primary and secondary flow, were decelerated as they entered the

junction and flowed into the daughter branches. Some values of the linear velocities at various points on the streamlines are given in Figure 2.

Velocity distributions at Re = 2.15 in the median plane of the bifurcation were computed from the measured distances (<0.3 mm) moved by the spheres in a given time across arbitrarily drawn lines in the parent and daughter tubes, and are shown in Figure 3. Wall shear rates were determined from the slope of the best-fit curves drawn through the experimental points of the velocity profiles.

It is evident that, as the flow approached the apex, the velocity profiles became blunted. At the entry and for 2 diameters downstream in the daughter tubes, the profiles were skewed towards the inner wall, where the shear rates (given in Figure 3) were markedly higher than those on the outer wall (Schroter and Sudlow, 1969; Schreck, 1972; Feuerstein et al., 1975; Talukder, 1976). Even greater differences in wall shear rates were observed at the higher Re where the respective values at the first position ($x_1 = x_2 = 1.24$ mm) in the daughter tubes were 3,000 and 16,700 sec^{-1} in the left branch, and 1,800 and 15,500 sec^{-1} in the right branch.

(2) Flow in Model Y-Bifurcations

Some investigators have reported flow separation and/or large secondary flow patterns on the outer walls of bifurcations of much greater diameters than those used in the present study (Hung and Naff, 1969; Fox and Hugh, 1970; Roach, Scott and Ferguson, 1972; Rodkiewicz and Roussel, 1973). In order to induce flow separation in the smaller bifurcations it was decided to extend the experiments to

Figure 3. Velocity distributions and wall shear rates (indicated by the numbers adjacent to the walls) in the same bifurcation as in Figure 2, at Re = 2.15. The distributions in the parent tube were measured at x_o = 0.52 mm and - 0.14 mm, and in the daughter tubes $x_1 = x_2$ = 1.24 mm and 1.91 mm.

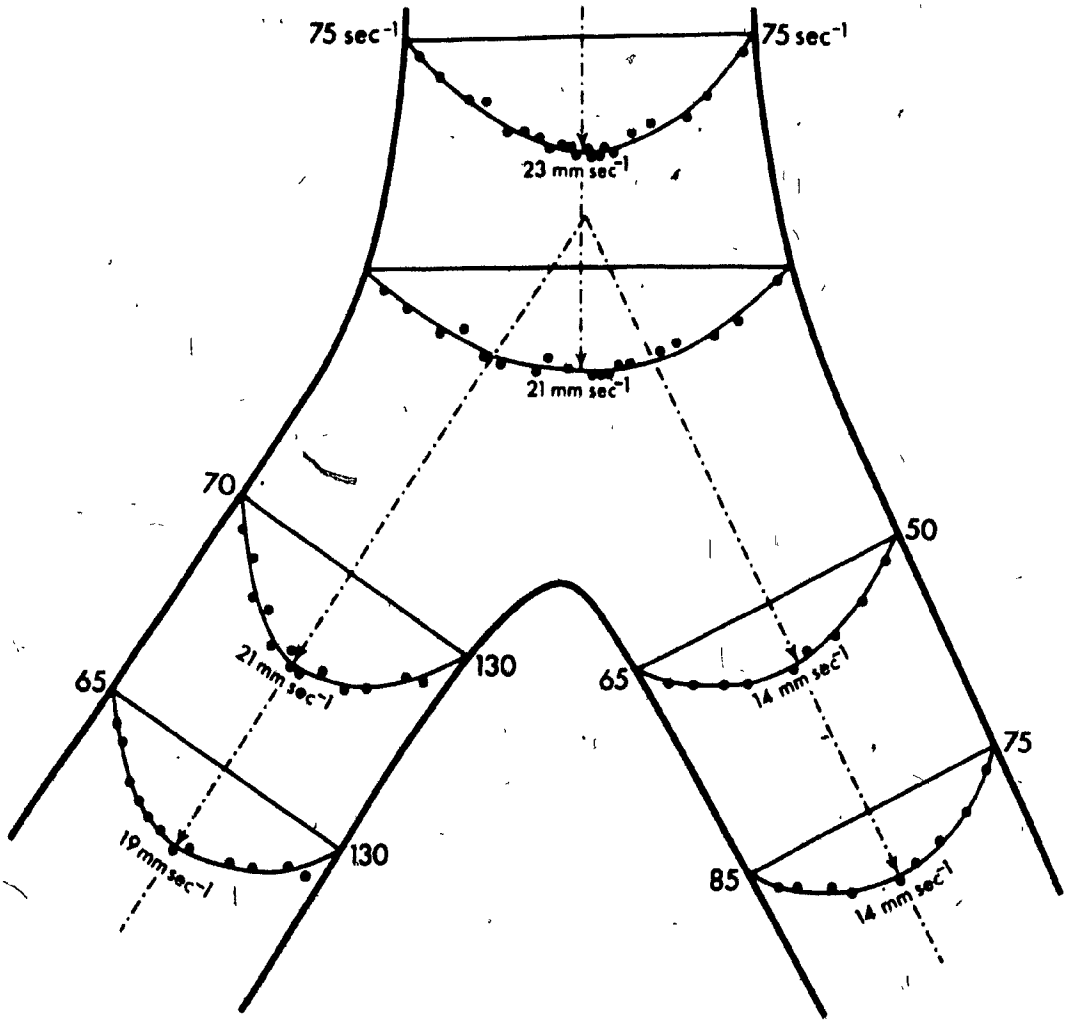
75 sec⁻¹
75 sec⁻¹
23 mm sec⁻¹
21 mm sec⁻¹
70
50
65
130
21 mm sec⁻¹
65
14 mm sec⁻¹
75
19 mm sec⁻¹
130
85
14 mm sec⁻¹

models having R_o and θ in the range of the dog mesentery bifurcations, but with smaller radii of curvature and $\alpha > 2$. Although branching vessels having such high α are not found in the vasculature (Caro et al., 1971; Gosling et al., 1971), it still seemed worthwhile to discover the manner in which flow separation developed as the flow rate was increased.

Experiments were carried out using carbon microspheres in benzyl alcohol flowing through a drilled bifurcation having $2R_o$ = 0.83 mm, α = 2.3 ($2R_1$ = 0.86 mm, $2R_2$ = 0.93 mm), $\theta_1 = \theta_2 = 30°$, with the radii of curvature 0.38 and 0.20 mm respectively (c.f. 1.72 and 2.11 mm in the dog mesentery bifurcation shown in Figures 2 and 3). Flow separation first occurred at Re ~ 80 ($\bar{U}_o$ ~ 530 mm sec^{-1}), and at somewhat higher Re spheres were seen in spiral vortices at the hips of the bifurcation upstream from the entry of the daughter branches. The general flow patterns are illustrated in Figure 4, where it can be seen that the vortex on the left is appreciably larger than that on the right, presumably because of the smaller radius of curvature of the left hand tube wall. It is also evident that spheres entering the vortex did so on streamlines (shown as the dashed lines in the Figure) which were part of the secondary flow, and some of which resembled those previously shown in Figure 2b.

Detailed studies of the development of the vortex were made by taking cine films at higher magnification, focussing on the flow patterns in the right half of the bifurcation. Figure 5 illustrates the sphere paths at Re = 83.7 and 154 ($\bar{U}_o$ = 555 and 1,030 mm sec^{-1} respectively). At the lower Re, secondary flow streamlines similar to those in Figure 2b were traced by spheres located above and below

Figure 4. General flow patterns, as indicated by the paths of carbon microspheres in benzyl alcohol in a model Y-bifurcation consisting of channels drilled into a polished epon resin block; R_o = 0.41 mm, R_1 = 0.43 mm, R_2 = 0.46 mm, Re = 176; $\overline{U}_o$ = 2.35 m sec^{-1}. The solid lines represent particle paths in the median plane of the bifurcation, and the dashed lines the secondary flow patterns and spiral vortices in the region of flow separation on the hips of the bifurcation. The reattachment points are indicated by the large arrows and the numbers give the particle velocities in mm sec^{-1} measured at the positions given by the thicker lines.

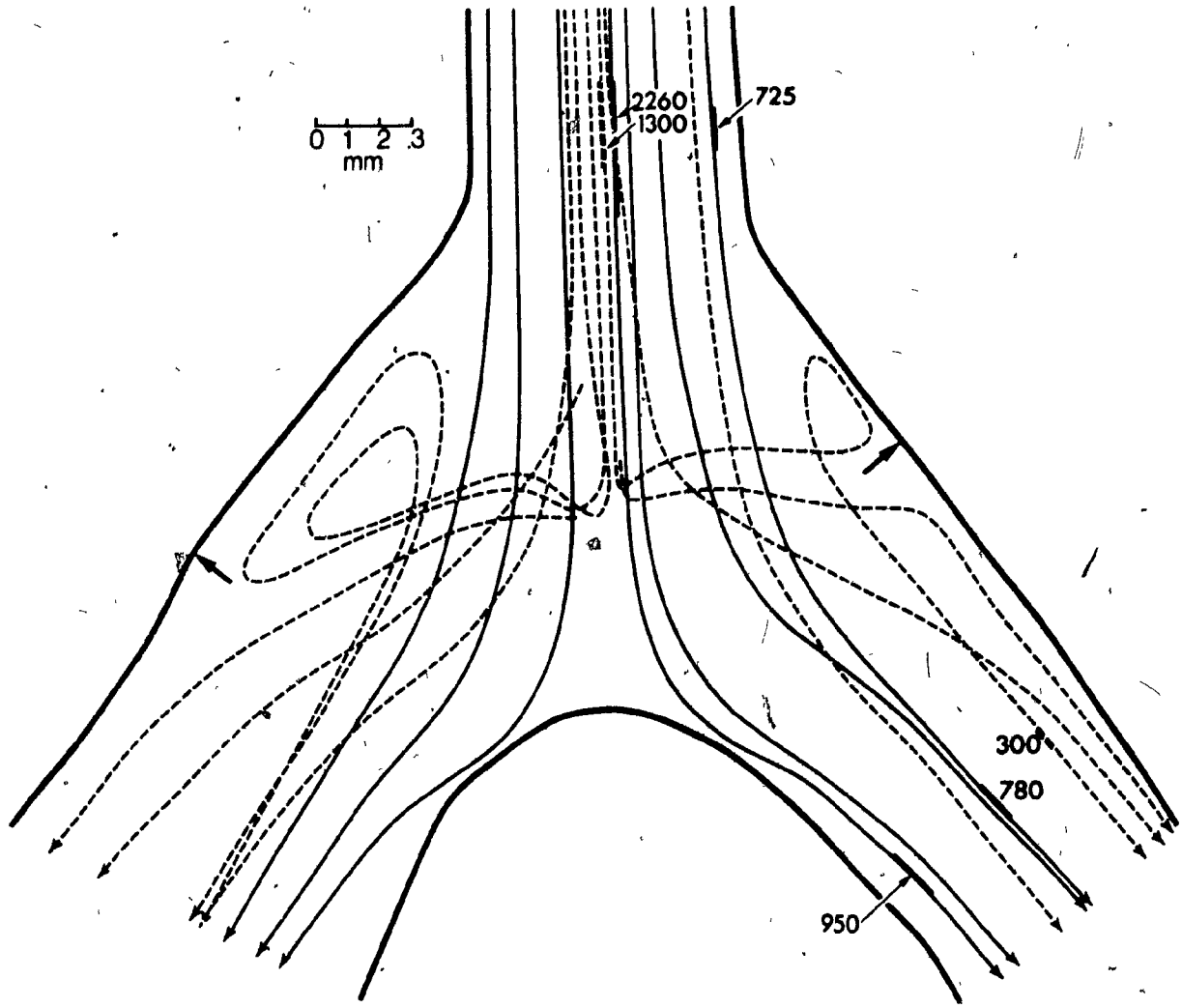
0 1 2 3
mm
2260
1300
725
300
780
950

Figure 5. Detailed flow patterns in the right half of the model bifurcation shown in Figure 4, proximal to the entry of the daughter branch; Re = 83.7, $\bar{U}_o$ = 555 mm sec^{-1}. (a): paths of 35 μm carbon microspheres in benzyl alcohol; (b): 15 μm spheres. The solid lines are particle paths in the primary flow in the median plane of the bifurcation, the dashed lines are paths in the secondary crossflow. No particles are seen in an area at the wall where, it is presumed, flow separation has occurred. Particle velocities are given in mm sec^{-1} at the positions indicated by the thicker lines.

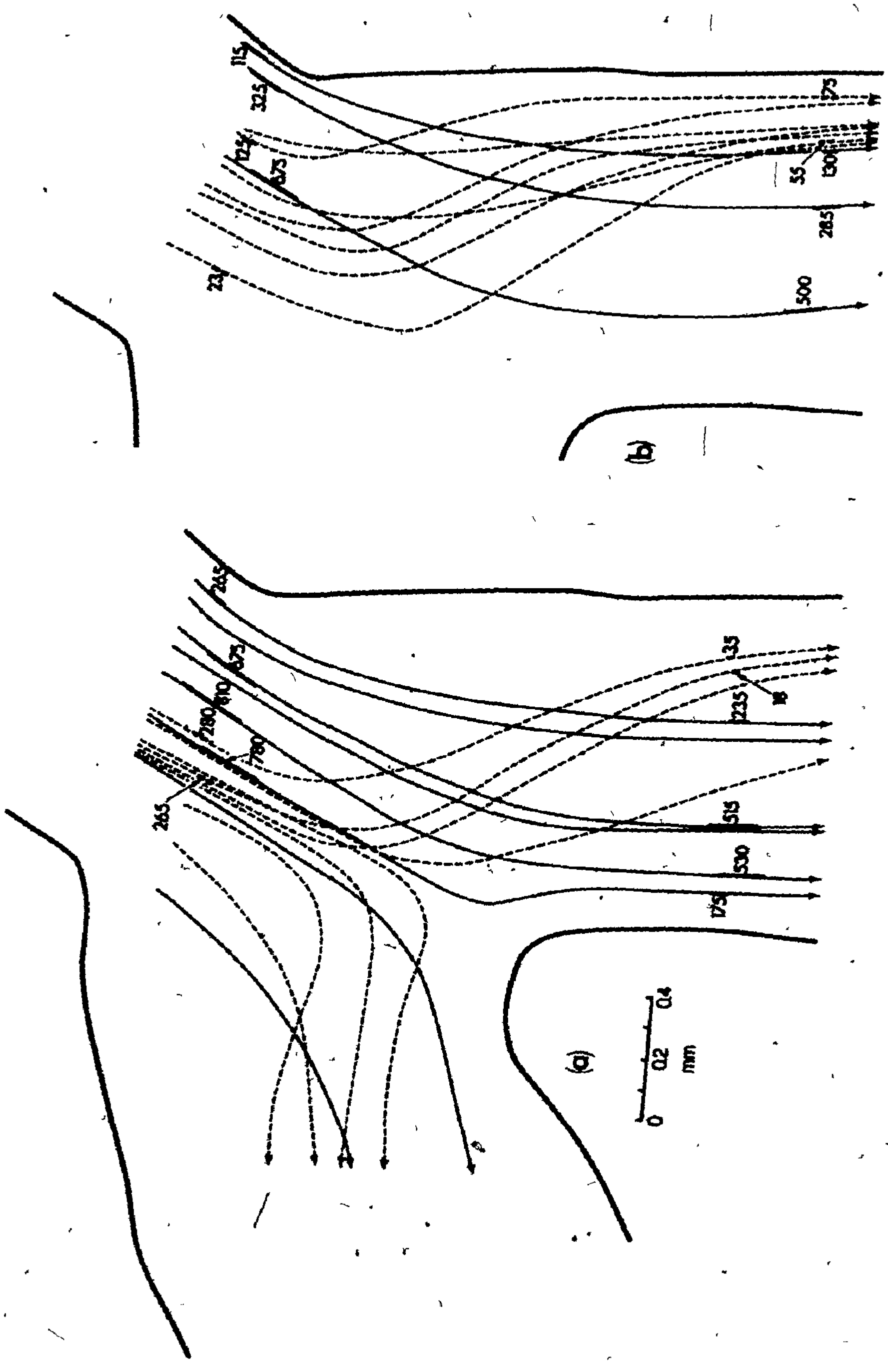
(a)
(b)
0 0.2 0.4
mm

the median plane which moved with velocities lower than others in the mainstream at comparable radial positions (Figures 5a and b). It is possible that flow separation had occurred in an area close to the tube wall just past the corner of the bifurcation, although no particles entered this region and no vortices were seen. In the animal bifurcation, by contrast, no flow separation was seen even at much higher Re (Figure 2b, Re = 133). Also striking were the differences in the paths of 15 and 35 μm spheres in the secondary flow. The former were able to move along streamlines which, judging by their velocities, came from positions closer to the parent tube wall and which crossed the primary flow further upstream from the entry of the daughter branch and approached closer to the outer wall than the 35 μm spheres.

As the flow rate was increased, the region of flow separation expanded, the secondary crossflow moved upstream and both 15 and 35 μm spheres were seen to flow through a series of triangular-shaped spiral vortices on streamlines located above and below the median plane having their origin in the middle of the parent tube (Figures 5c and d). As at the lower Re, so at Re = 154, the 15 μm spheres were able to approach the outer wall on streamlines apparently closer to the upper or lower tube wall than the 35 μm spheres (e.g. the lowest velocities were 210 and 295 mm sec^{-1} for 15 and 35 μm spheres respectively). This resulted in the presence of the smaller spheres in orbits or varying size throughout the vortex region of separated flow, whereas the larger spheres were only seen in orbits closer to the reattachment point (indicated by the large arrow).

Figure 5 (continued): Re = 154, $\bar{U}_o$ = 1.03 m sec^{-1}; (c): 35 μm spheres, (d): 15 μm spheres. Particles in the secondary cross-flow enter spiral vortices in the region of flow separation. The arrows show the position of the reattachment point.

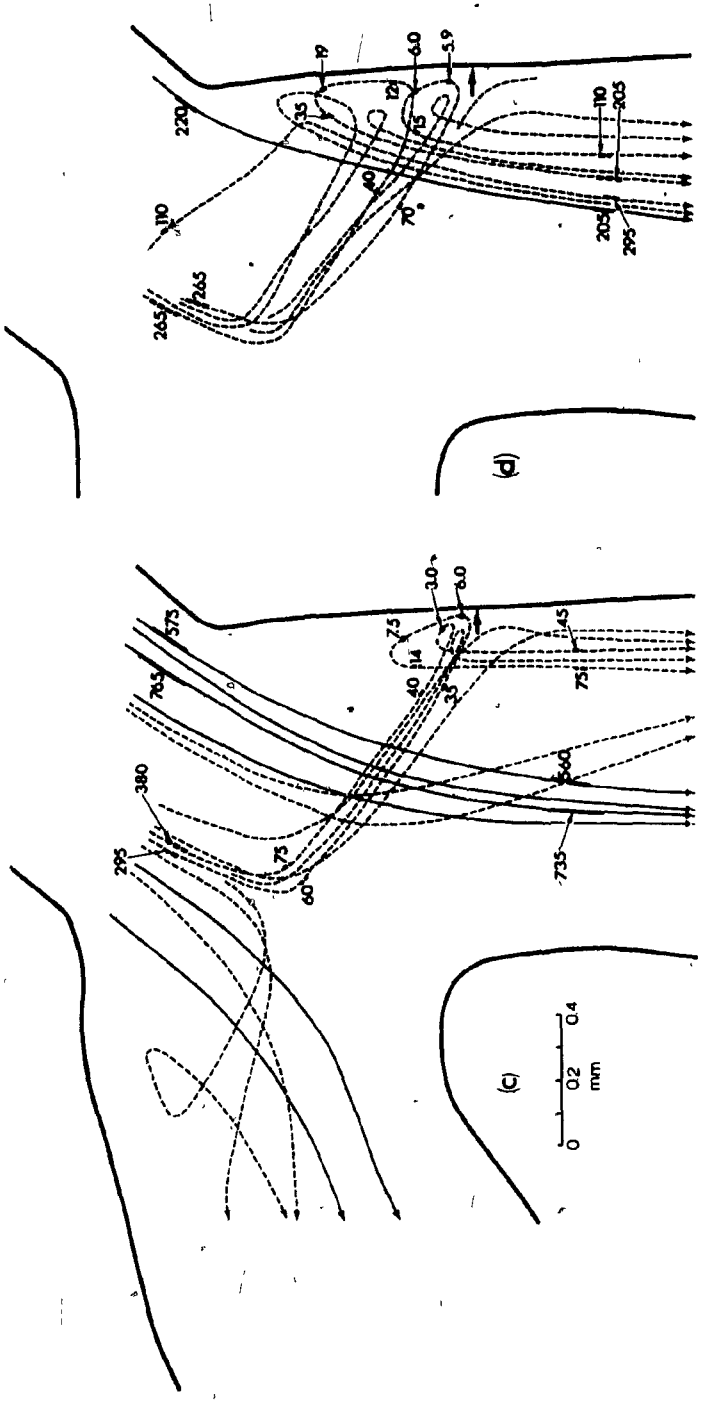
(d)
(c)
0
0.2
0.4
mm

Particle velocities, given on several of the streamlines in the Figures, decreased as the spheres approached the vortex on paths which were visually observed to be far out of the median plane. The velocities were a minimum as the particles entered the reverse flow region, when they were judged to be closer to the median plane. The velocities now increased again, at first slowly during reverse flow parallel to the tube wall, then more rapidly as forward motion was resumed, at which point they appeared again to be far out of the median plane.

As a consequence of the low velocities within the vortex, the residence times of spheres in orbit (from 15 to 60 m sec) were long compared to the time taken by a particle near the vortex boundary, or that of one travelling with the mean tube velocity, to traverse its length (4 m sec and 0.3 m sec respectively).

(3) Open T-Bifurcations

The flow patterns in dilute benzyl alcohol suspensions of 15 and 32 μm polystyrene spheres were observed in a symmetric 180° (T-) bifurcation having $R_o = R_1 = R_2 = 0.358$ mm at tube Reynolds numbers Re from 1 to > 200. The radii of curvature of the outer walls, as in the model Y-bifurcations, were small, being < 0.15 R_o. As illustrated in Figure 6a for Re = 2.9, at the lower flow rates, the particle paths traced from cine films were parallel to the tube walls, the streamlines in the junction dividing symmetrically about the parent tube axis. The measured particle velocity distribution in the median plane of the parent tube was found to be parabolic to within 0.2 tube diameters of the junction.

Figure 6. The paths of 15 and 32 μm diameter polystyrene spheres in benzyl alcohol flowing through a symmetric T-bifurcation; $R_o = R_1 = R_2 = 0.358$ mm. (a): $\bar{U}_o = 18.3$ mm sec^{-1}, Re = 2.9; particle paths in the junction divide symmetrically about the parent tube axis. (b): $\bar{U}_o = 119$ mm sec^{-1}, Re = 15.5; secondary flow patterns appear, as shown by the dashed lines which represent the paths of spheres travelling above or below the common median plane of parent and daughter tubes. The numbers in the diagram refer to particle velocities, in mm sec^{-1}, measured at the positions given by the thicker lines.

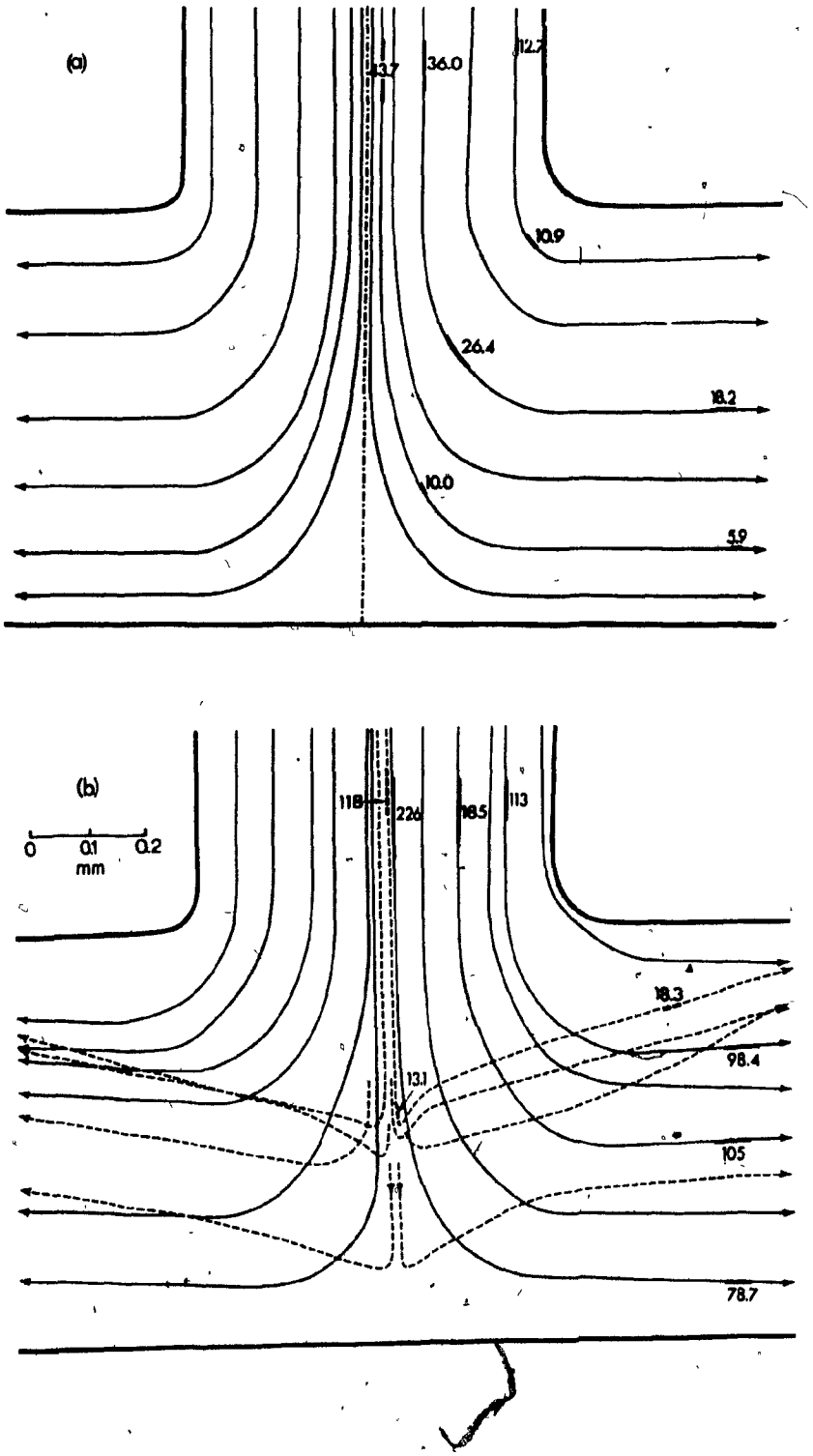
(a)
13.7
36.0
12.7
10.9
26.4
18.2
10.0
5.9
(b)
0
0.1
0.2
mm
118
22.6
18.5
113
18.3
98.4
13.1
105
78.7

When the flow rate was increased, secondary flow patterns appeared, as shown by the dashed streamlines in Figure 6b at Re = 15.5 ($\bar{U}_o$ = 119 mm sec^{-1}). The spheres travelling on such streamlines were not in the median plane normal to the viewing axis, but, as in the Y-bifurcations, were visible because of the appreciable depth of focus (± 70 μm) existing at the relatively low magnifications used (≤ 50×). Again, they were recognized by their velocities, which were lower than those of spheres at the same apparent radial distance but flowing in the median plane. At first the secondary flow patterns were only seen with spheres whose apparent radial position in the median plane was close to the tube axis. The velocities of these particles decreased as they entered the junction and were seen to go out of focus and thus further out of the median plane until they moved parallel to the viewing axis and appeared to be at a standstill. They then reversed direction while at the same time flowing into the daughter branch, the projection of their path crossing that of spheres in the median plane, and their velocity in the axial, X-direction, increasing with time.

A further increase in flow rate led to larger and more pronounced secondary flow patterns, similar to those shown in Figure 6b, which involved spheres whose apparent radial position in the median plane was further from the tube axis and whose flow into the branches took them much closer to the corner of the bifurcation.

Observations of flow in the T-bifurcation were made at Re up to 205, corresponding to $\bar{U}_o$ = 1.58 m sec^{-1}; but no region of flow separation and no vortex was seen. At such Re, even the maximum attainable camera framing speed of 6,000 sec^{-1} was insufficient to

capture the faster travelling spheres on the cine film. At this time, it was noted that by partially occluding one daughter branch of the T, a vortex developed at its entry and, depending on the degree of closure, flow separation occurred at much lower Re. A study of such flows was therefore undertaken; they are known to occur in the circulation as a result of the growth of atherosclerotic plaques in the daughter branch of a bifurcation (Lallemand et al., 1972; Najafi et al., 1975).

(4) Partially Occluded T-Bifurcations

(a) Degree of occlusion and Re. By using a variable closure clamp on the outflow polythene tubing attached to one of the daughter branches, the flow was slowly and progressively occluded until a vortex was just seen to form. The degree of occlusion, defined as $(1 - Q_2/Q_1)$, was obtained by measuring the volume rate of flow out of the two daughter branches and plotted against parent tube Re at which a vortex just formed, as shown in Figure 7. It is evident that, at low Re, almost total closure of the branch was necessary for a vortex to form (>99% of the volume flow passed through the open branch). With increasing flow into the parent branch, the vortex formed at rapidly decreasing degrees of occlusion: thus, at Re = 32, a quarter of the total flow passed through the partially obstructed branch.

(b) Vortex size, flow patterns and Re. The formation and growth of spiral vortices at the entry of a partially occluded branch at a constant degree of occlusion = 0.998 was observed by tracing particle paths in a mixed, dilute suspension of 15 and 32 μm spheres

Figure 7. The degree of occlusion, defined as $(1 - Q_2/Q_1)$, where Q_1 and Q_2 are the volume flow rates through open and partially occluded daughter branches, plotted against the parent tube Reynolds number at which a vortex first forms. At low Re, almost total closure of daughter branch #2 was necessary before flow separation occurred; at Re = 32, a quarter of the total flow passed through the partially occluded branch.

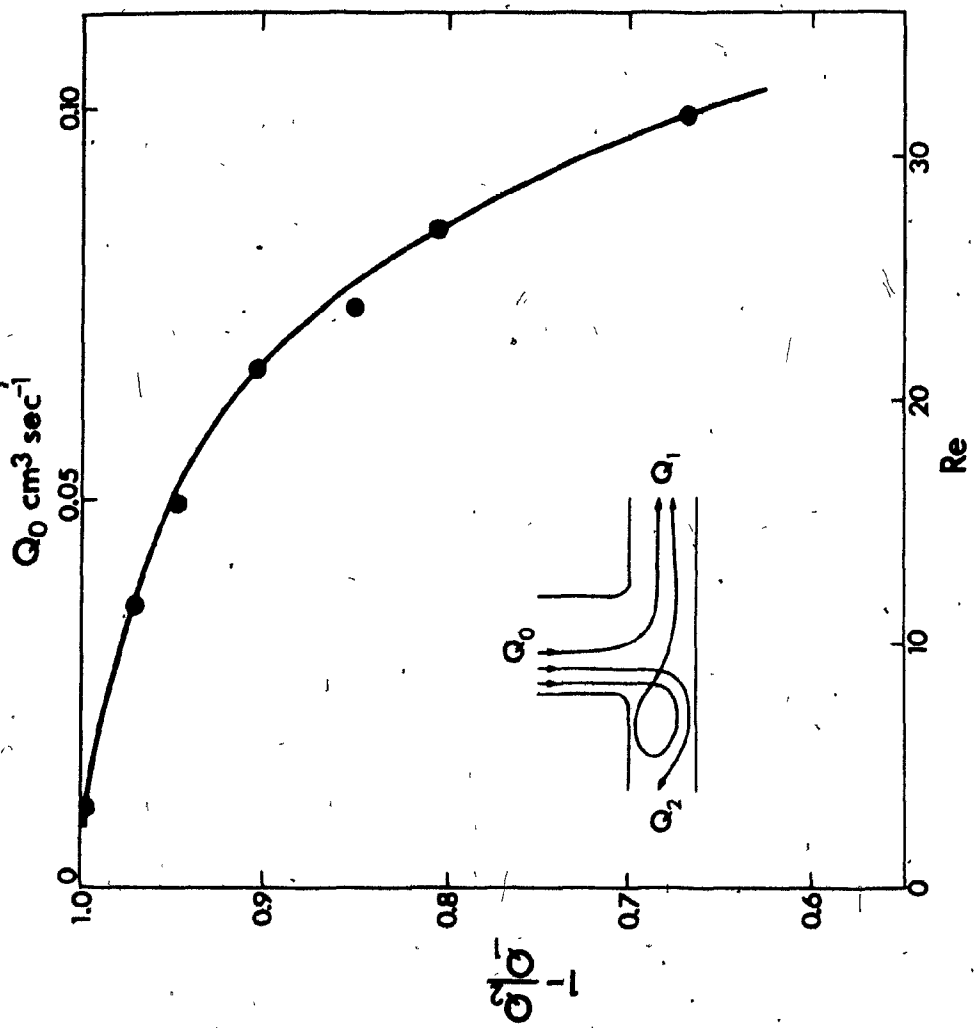
Q_0 cm^3 sec^{-1}
0
0.05
0.10
Re
0
10
20
30
$\frac{\sigma_1}{\sigma} - 1$
1.0
0.9
0.8
0.7
0.6
Q_0
Q_1
Q_2

at progressively increasing Q_o. In contrast to flow through the open T-bifurcation, the streamlines in the partially occluded system no longer divided symmetrically about the parent tube axis but were deflected towards the obstructed branch. A vortex was first seen at a parent tube Re = 3.3 ($\bar{U}_o$ = 25.2 mm sec^{-1}), and as shown by the sphere paths plotted in Figure 8a, it was situated at the entry of the obstructed branch with its center lying close to the tube axis. Only 15 μm spheres were seen to enter the vortex from streamlines close to the wall of the parent tube, after circulating through one or two orbits the particles rejoined the mainstream in the open branch. The 32 μm spheres all flowed directly into the open branch, as shown by the dashed lines in the Figure. It was evident also that the particle paths traced near the parent tube wall followed streamlines which were often out of the median plane normal to the viewing axis. Thus, in Figure 8a, the sphere on the 5th streamline from the wall at an apparent $R = 0.84R_o$ flowed into the partially occluded branch with a velocity of 11.8 mm sec^{-1}, whereas the faster moving particle on the 4th streamline at $R = 0.86R_o$ flowed into the open branch with a velocity of 13.0 mm sec^{-1}. Since the particle velocity distribution $u_o(R)$ was known to be parabolic close to the junction, the sphere radial positions could be calculated from the relation

$$\frac{u_o(R)}{u_o(0)} = \left(1 - \frac{R^2}{R_o^2}\right),$$

using the measured particle centerline velocity $u_o(0)$. The results showed that, as was visually evident from the cine film, those spheres which entered the vortex and some of those continuing into the obstructed

Figure 8. Particle paths as in Figure 6 in a T-bifurcation in which the left hand branch is almost totally occluded, $(1 - Q_2/Q_1) \leq 0.998$, showing the formation and growth of spiral vortices with increasing Re. (a): $\bar{U}_o = 25.2$ mm sec^{-1}, Re = 3.3; a vortex just forms and only 15 μm spheres entering the junction along streamlines close to the tube wall (solid lines) flow into the vortex. The 32 μm spheres (dashed lines) all flow directly into the right hand, open branch. The numbers refer to particle velocities at the positions indicated and the thick arrow gives the separation point of the flow.

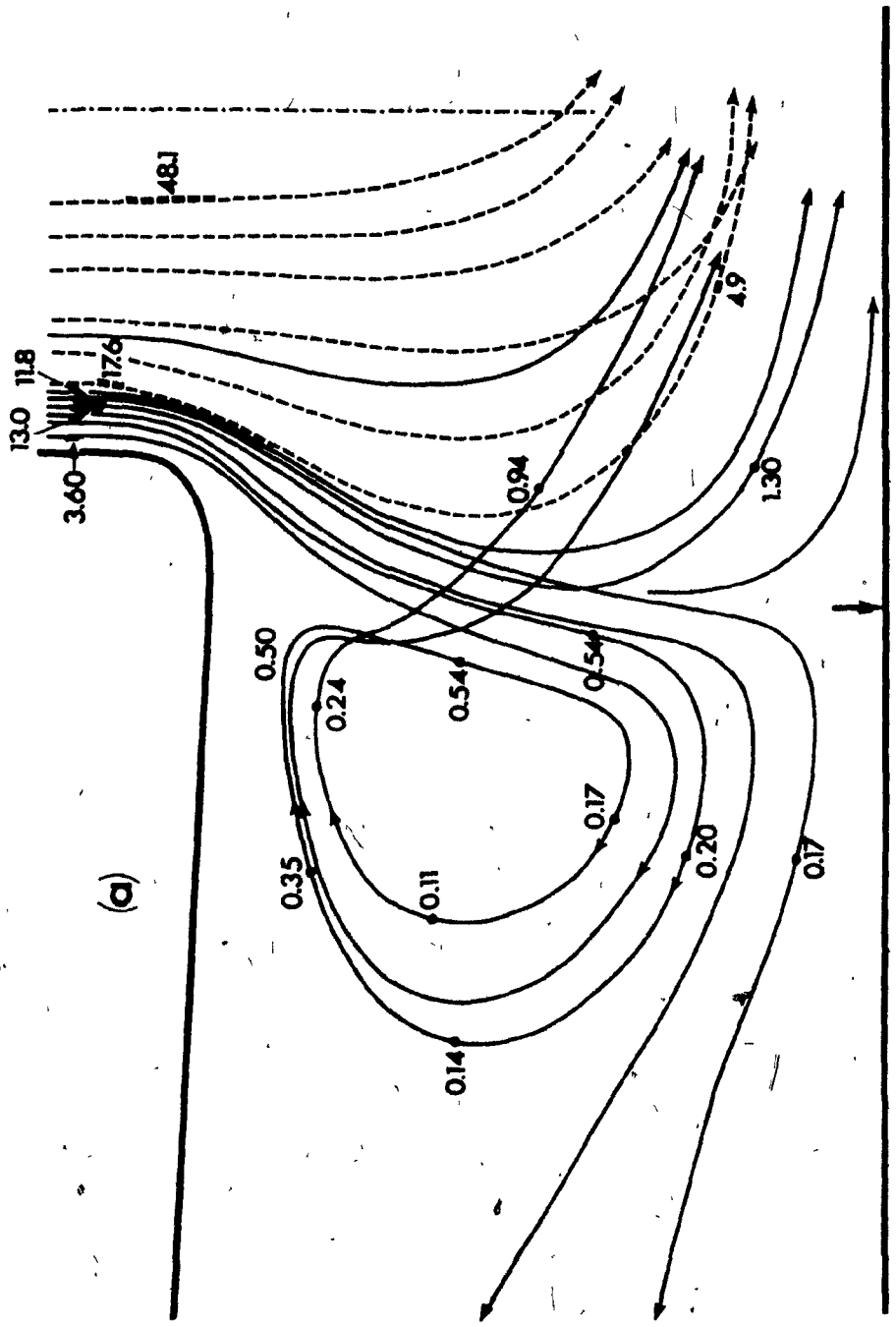
48.1
17.6
11.8
13.0
3.60
0.94
4.9
1.30
0.50
0.24
0.54
0.54
0.17
0.35
0.11
0.20
0.17
0.14
(a)

Figure 8 (continued). (b) and (c): respective paths of 15 and 32 μm spheres at $\overline{U}_o$ = 75.5 mm sec^{-1}, Re = 9.8. Here, the streamline dividing flow into the two branches has moved away from the parent tube wall and 32 μm spheres enter the vortex. The dashed lines in (c) represent spheres which flowed into the junction far above or below the median plane (c.f. Figure 10). The numbers refer to particle velocities at the positions indicated and the thick arrows give the separation point of the flow.

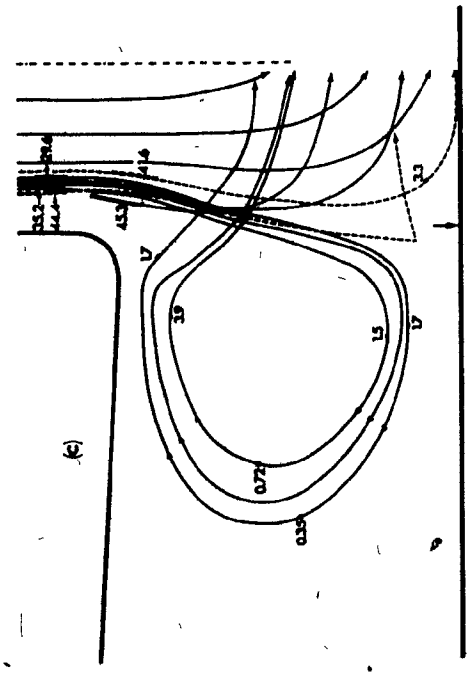
(c)
0.72
0.35

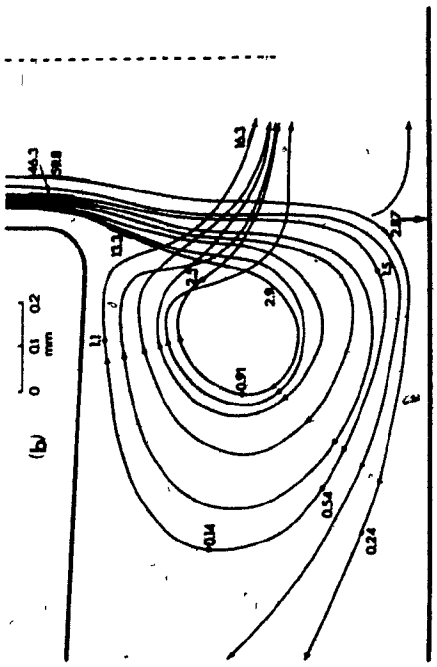
0.2
0.1
mm
0
(b)
0.91
0.14
0.54
0.24

branch, travelled on streamlines lying out of the median plane. The first and second streamlines from the wall in Figure 8a were estimated to be $0.17R_o$, or 58 μm above or below the median plane, and while the 4th streamline lay in the median plane, the 5th streamline was $0.26R_o$, or 95 μm out of the median plane. Those sphere paths shown entering the open branch in Figure 8a were situated in the median plane of both parent tube and junction. The streamline dividing particles entering the vortex from those flowing through the obstructed branch was located at $R = 0.94R_o$, and that which divided flow into the two branches at $R = 0.88R_o$. No 32 μm spheres were traced at positions close to the parent tube wall.

Although flowing into the junction while out of the median plane, the spheres which entered the vortex moved into focus as they reached the partially occluded branch with their velocity markedly reduced. They now appeared to be in, or close to the median plane as they moved into the reverse and radial flow portions of the orbits of the vortex. Then, as they resumed forward motion with increasing velocity, they again moved out of focus, crossing above or beneath the mainstream in the junction and flowing into the open branch. Particle velocities varied widely; for instance, the sphere which entered the junction on the second streamline with a velocity of 6.8 mm sec^{-1} was moving at only 0.14 mm sec^{-1} at its furthest point into the branch on the outermost orbit, accelerating and decelerating as it circulated in the second, smaller orbit before rejoining the mainstream at a progressively increasing velocity. The residence time τ in the vortex was 12.7 sec — very large compared to the time $\bar{t}$, taken by a particle having a mean linear velocity $\bar{U}_o$ to travel

past the vortex. In fact such a sphere would by then have moved a distance 330 mm downstream into the open branch.

The dimensions of the vortex (Figure 9) and the residence times for spheres circulating on the outermost orbits are listed in Table 2. The vortex size is given in terms of the axial distance x_{2M} of the outermost orbit and the distance x_{2S} of the separation point dividing the streamlines, both measured from the midpoint of the T, as well as the apparent width ΔR of the outermost orbit in terms of the radial coordinate of the branch.

The size of the vortex increased with increasing flow rate, both in length, approximately given by $(x_{2M} - x_{2S})$, as well as in width, ΔR. At the same time the whole vortex region moved upstream towards the open branch with the streamline dividing flow into the two branches, and that dividing flow into the vortex from that through the obstructed branch, moving closer to the parent tube axis. This resulted in larger orbits and in the presence of 32 μm spheres in the vortex, although as illustrated in separate tracings for the two sizes of spheres in Figures 8b and c and Figures 10a - d, only the 15 μm spheres could enter the vortex on streamlines close to the tube wall and circulate in the smaller as well as in the larger orbits.

Upon increasing Re from 3.3 to 9.8 ($\bar{U}_o$ = 75.5 mm sec^{-1}), the dividing streamlines moved from 0.88 to $0.77R_o$, and from 0.94 to $0.84R_o$, respectively. As illustrated in Figures 8b and c, there were again large changes in particle velocities, and the residence times although shorter were still very large compared to the calculated $\bar{t}$ (Table 2). When Re was increased to 16.2 ($\bar{U}_o$ = 125 mm sec^{-1}) the vortex size increased further, with the streamline dividing flow into the vortex from that through the obstructed branch moving away from the wall to

Figure 9. Coordinates used to describe flow and the dimensions of the vortex in a partially occluded T-bifurcation.

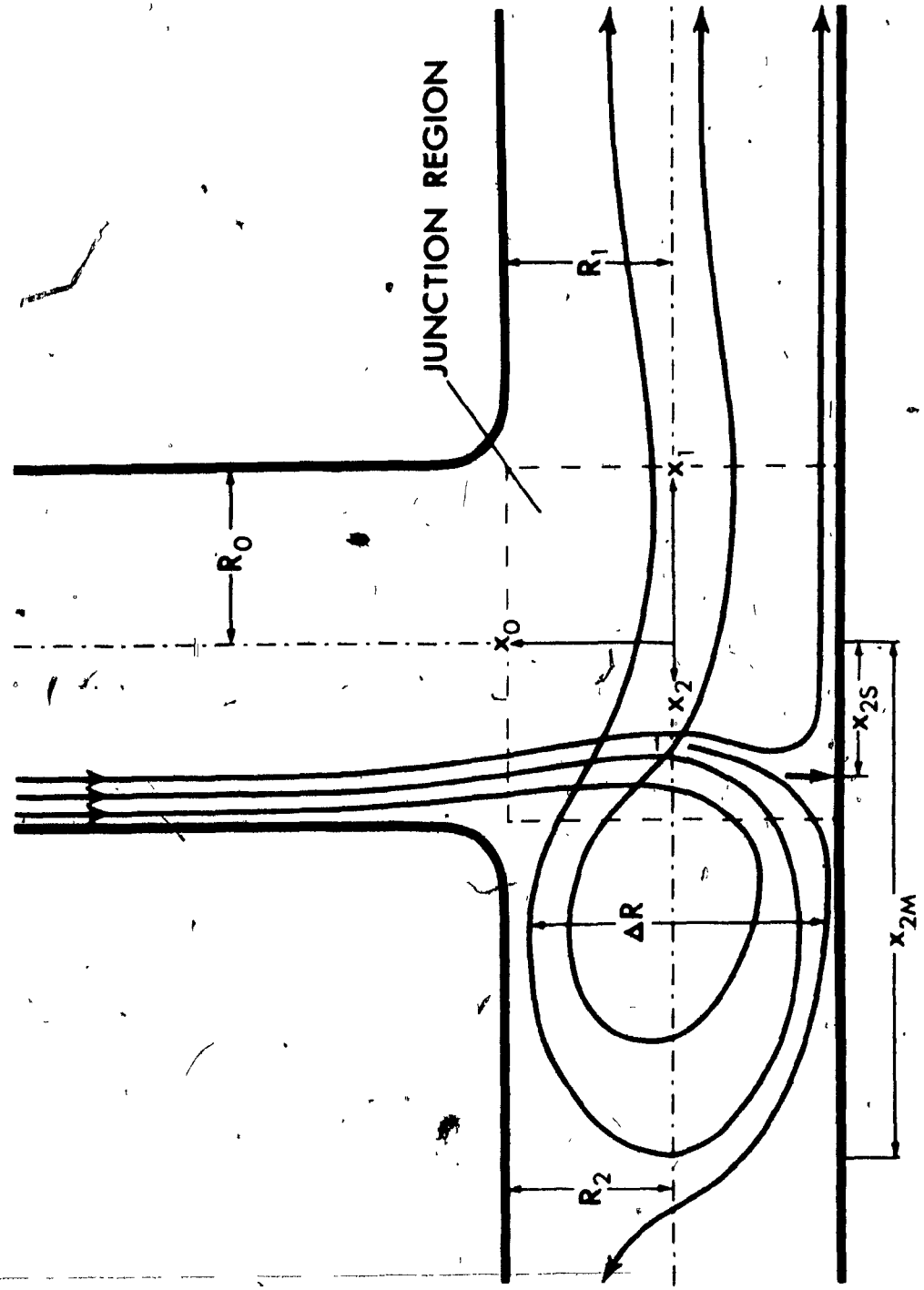
JUNCTION REGION
R_1
R_0
x_1
x_0
x_2
x_{2S}
ΔR
x_{2M}
R_2

TABLE 2

VORTEX DIMENSIONS AND PARTICLE RESIDENCE TIMES

$\bar{U}_o$ mm sec^{-1}	Re	Sphere diameter μm	Vortex dimensions[a] x_{2M} mm	x_{2S} mm	$(x_{2M} - x_{2S})$ mm	ΔR mm	τ[c] sec	$\bar{t}$[d] sec
25.2	3.3	15	0.92	0.56	0.36	0.55	12.7	0.022
		32[b]	-	-	-	-	-	-
75.5	9.8	15	0.98	0.34	0.64	0.61	3.00	0.008
		32	0.92	0.42	0.50	0.53	2.08	0.007
125	16.2	15	1.02	0.28	0.75	0.61	2.73	0.005
		32	1.03	0.29	0.75	0.60	2.62	0.005
177	22.9	15	1.00	0.14	0.87	0.63	1.63	0.004
		32	0.82	0.15	0.67	0.60	0.65	0.003

a) Defined in Figure 9; they refer to the largest orbits observed

b) No 32 μm spheres seen in the vortex

c) Maximum value of the residence time

d) $\bar{t} = \Delta R/\bar{U}_o$

$R = 0.82R_o$. At this higher flow rate there appeared smaller spiral orbits situated close to or in the junction which are shown by the dashed lines in Figures 10a - d. Particles which circulated in such orbits left the parent tube on streamlines close to the median plane (i.e. at higher velocities than those spheres which entered the other orbits of the vortex). Once in the junction they went out of focus, their velocity decreasing rapidly until they reversed direction and moved into an orbit of small diameter, after which they rejoined the mainstream in the open branch. At the highest Reynolds number studied, Re = 22.9 ($\bar{U}_o$ = 176 mm sec^{-1}) the vortex had now moved well into the junction area (x_{2S} = 0.14 mm) and the above mentioned smaller spiral orbits had grown in size and were located above or below the other orbits of the vortex (Figures 10c and d). In contrast to the results obtained at lower Re, the largest orbits of the 32 μm spheres were appreciably shorter than those of the 15 μm spheres.

(c) Vortex size, flow patterns and degree of occlusion.

A study was also made of the development and growth of the vortex at a given flow rate as the degree of occlusion was increased. Typical flow patterns observed at Re = 37.6 with Q_2/Q_1 = 0.40 and 0.0032 respectively, are shown in Figures 11a and b. It is apparent that it is the secondary flow patterns first described above in the case of the open T-bifurcation (Figures 6a and b) that develop into a small spiral vortex situated not far from the corner of the partially occluded branch. Polystyrene spheres entering the vortex rejoined the mainstream flowing out of this branch, unlike the flow illustrated in Figures 8 and 10 at higher Q_2/Q_1. Upon increasing the degree of occlusion, however, the spheres entering the vortex on streamlines out

Figure 10. Growth of spiral vortices in the same system as in Figure 8, at higher Re. The paths of the 15 μm spheres (a) and 32 μm spheres (b) are drawn separately $\overline{U}_o$ = 125 mm sec^{-1}, Re = 16.2.

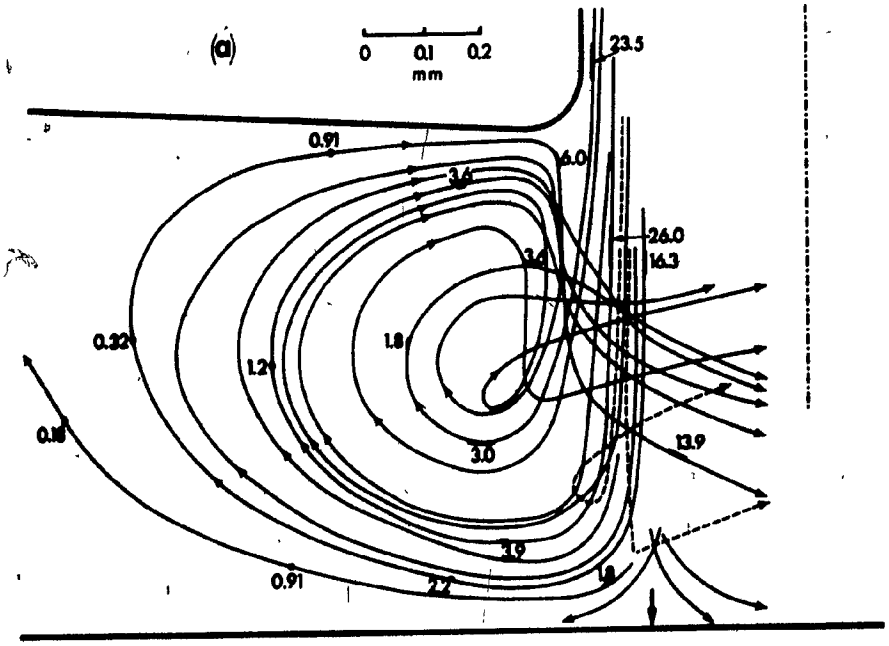
(a)
0
0.1
0.2
mm
23.5
0.91
6.0
3.6
26.0
16.3
3.4
0.32
1.8
1.2
0.18
3.0
13.9
3.9
0.91
2.7
1.8

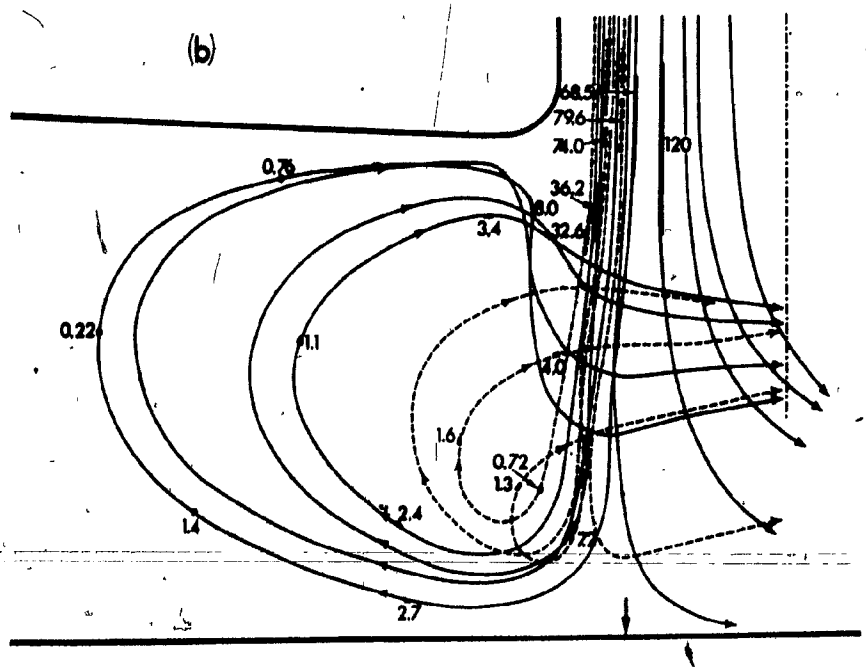
(b)
68.5
79.6
76.0
120
0.78
36.2
8.0
3.4
32.6
0.22
11.1
4.0
1.6
0.72
1.3
2.4
1.4
2.7
2.7

Figure 10 (continued). (c), 15 μm spheres and (d), 32 μm spheres; $\overline{U}_o$ = 176 mm sec^{-1}, Re = 22.9. The dashed lines represent the paths of spheres which circulated in small spiral orbits lying far out of the median plane, in contrast to the other, larger orbits, portions of which lie close to the median plane of the daughter branch #2.

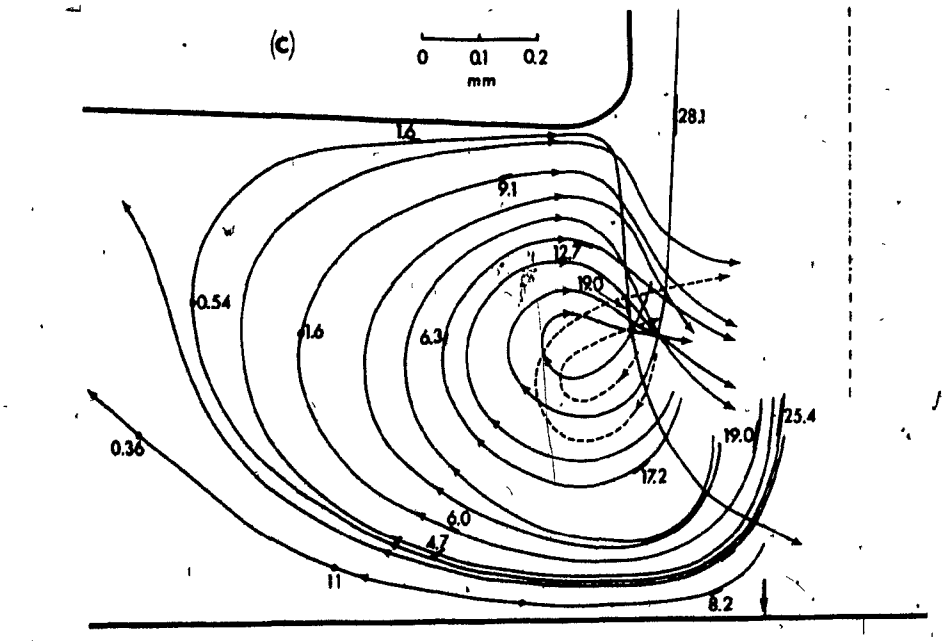
(c)
0 0.1 0.2
mm
28.1
1.6
9.1
12.7
19.0
0.54
1.6
6.3
0.36
25.4
19.0
17.2
6.0
4.7
11
8.2

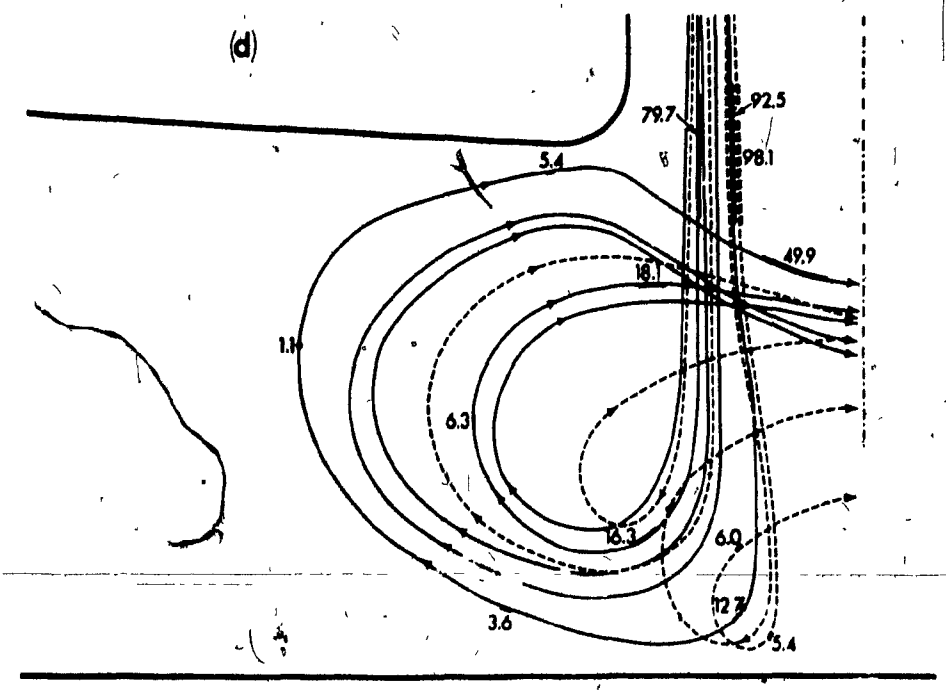
(d)
79.7
92.5
98.1
5.4
49.9
18.1
1.1
6.3
16.3
6.0
12.7
3.6
5.4

Figure 11. Growth of a vortex, as shown by the paths of 32 μm spheres at Re = 37.6 in the T-bifurcation of Figures 6-8 and 9 as the degree of occlusion of the left hand daughter branch was increased from $1 - Q_2/Q_1 = 0.60$ in (a) to 0.996 in (b). In (a) it is the spheres on streamlines lying out of the median plane (shown dashed, c.f. Figure 6) which enter a small vortex and flow out of the partially occluded branch. In (b) the vortex is similar to that in Figures 8 and 10 and spheres entering it flow back into the open branch.

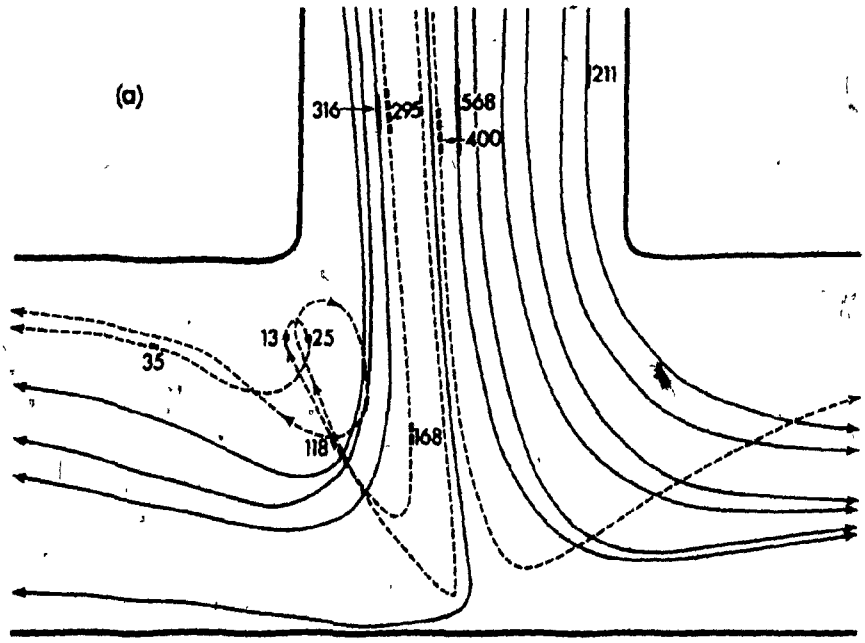
(a)
316
295
568
400
211
13
25
35
118
168

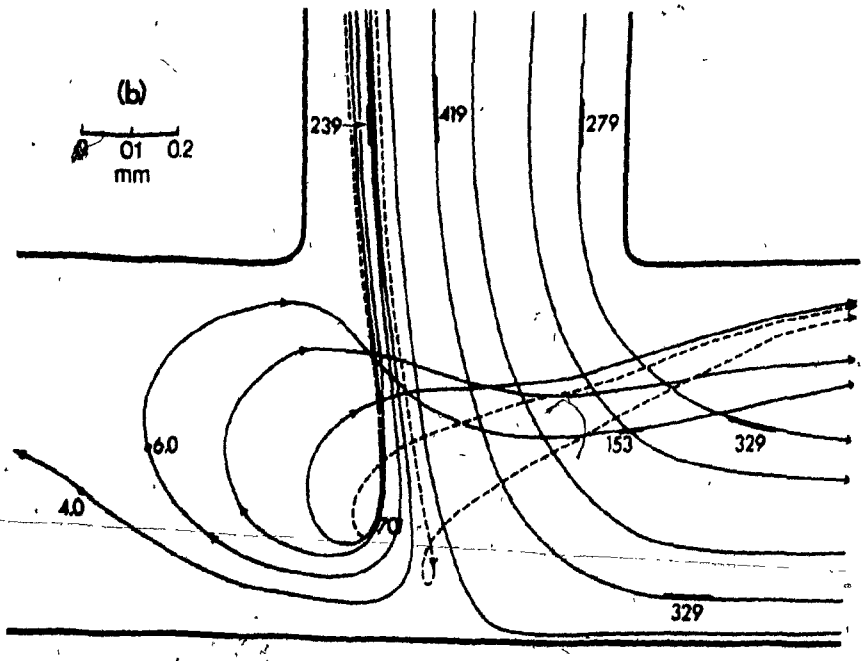
(b)
0
01
0.2
mm
239
419
279
6.0
4.0
70
153
329
329

of the median plane of the parent tube, flowed out of the open branch, and the streamlines dividing flow into the two branches were shifted toward the partially occluded vessel (Figure 11b).

When Q_2/Q_1 was increased further, the dividing streamline moved even closer to the partially occluded branch, and fewer and fewer spheres were seen to enter the vortex. Finally, when the branch was totally occluded, particles were no longer seen orbiting within a vortex. Instead, they travelled on streamlines which just entered the occluded branch, then reversed direction and moved into the open branch.

DISCUSSION

The above described experiments represent the initial phase of an investigation of the flow properties of suspensions in bifurcations, being restricted to a study of the behavior of small rigid spheres. Ultimately, the work is aimed at understanding the effects of branching flows on individual corpuscles in human blood. For this reason, bifurcations with tube diameters less than 1 mm were used so that the movements of suspended particles could be observed and photographed through a microscope. This, in turn limited the maximum Reynolds numbers which could be reached, given the suspending fluid viscosity and the flow system employed, and consequently the degree to which secondary flows and, in the limit, flow separation were present.

It was not surprising, therefore, to find that in the dog mesentery bifurcations having outer walls with high radii of curvature, only a moderate secondary flow developed even at the highest Re (≈ 150).

There was no separation of the streamlines from the walls distal to the bends of the bifurcation. Clearly, in these, the larger arterial bifurcations of the mesentery (Table 1) where, in vivo, Re is unlikely to exceed 80 (McDonald, 1974) there will be no large effects due to secondary flow. Even in models of the major human arterial bifurcations, it has been noted that secondary flows, while appreciable at Re = 800, do not result in flow separation (Feuerstein et al., 1976).

At the entry of the daughter branches, the wall shear rates were found to be significantly higher at the inner than at the outer walls, in accord with the results of others in fluid (Talukder, 1975; Feuerstein et al., 1976) and in airway systems (Schroter and Sudlow, 1969; Schreck, 1972).

When, however, the radii of curvature became much smaller than the parent tube diameter, and the area ratios increased to abnormally high values ($\alpha = 2$), a pronounced secondary crossflow was observed. At Re > 80, flow separation occurred, with a region of backflow at the outside wall in which particles were seen to move in spiral vortices. The suspension which flowed through this region, vacated by the mainstream, came from areas close to the upper and lower walls at the center of the parent branch, slowly crossing the streamlines of the primary flow and moving laterally toward the outer tube wall (Brech and Bellhouse, 1973).

In the T-bifurcations, despite the small radii of curvature and the 90° angle of the bend, no flow separation was observed unless one of the daughter branches was partially occluded. A secondary crossflow, which moved from the center of the junction region across the mainstream into the daughter branches (Figure 6b), was detected in the unoccluded bifurcation already at Re = 15. This, it was found,

developed into a spiral vortex when one daughter branch was moderately occluded ($Q_2/Q_1 = 0.4$). When, however, the degree of occlusion was substantially increased, the streamlines entering the vortex originated from fluid close to the parent tube wall on the side of the obstructed branch (Figure 11b).

In both T- and Y-bifurcations, the streamlines traced by the suspended spheres depended on sphere diameter. For instance, in the Y-bifurcation only the 15 μm spheres were seen on those streamlines which filled the upper, proximal area of the vortex (Figure 5) and whose velocities were lower than any followed by the 35 μm spheres. In the T-bifurcation, only 15 μm spheres were seen in the vortex at the lowest Re: the 32 μm spheres all flowed into the junction at radial distances $< 0.94R_o$, that of the dividing streamline. At higher Re, while there were 32 μm spheres in the vortex, only the 15 μm spheres circulated in the inner orbits, which originated in streamlines close to the parent tube wall.

This effect presumably, is in large part due to the mechanical exclusion of particle centers at radial distances greater than one sphere radius from the tube wall. In the parent tube of the T-bifurcation, this would have restricted the 32 μm spheres to radial distances $R < 0.955R_o$ and the 15 μm spheres to $R < 0.979R_o$. In addition, the effect of fluid inertia, known to result in the inward radial migration of rigid spheres in Poiseuille flow (Brenner, 1966; Karnis et al., 1966; Cox and Hsu, 1976), should be considered. The measured rates of migration have been found to be proportional to tube Reynolds number, the third power of particle to tube radius and to the radial distance from the equilibrium position at $R \approx 0.6R_o$

(Segré and Silberberg, 1962). Calculations based on the empirically derived equation for radial migration (Yu and Goldsmith, 1973, see also Appendix B) show that, in the 20 mm entrance length of the present system, a 32 μm sphere would, at the lowest Re = 3.3 migrate inward 2 μm from $0.955R_o$ to $0.950R_o$, whereas a 15 μm sphere would only drift 0.4 μm inward from $0.979R_o$ to $0.978R_o$. At the highest Re = 22.9, however, the 35 μm particle would be expected to migrate inward by 20 μm reaching $R = 0.896R_o$, still within the region where streamlines entered the vortex.

A similar exclusion of larger particles from streamlines close to a boundary was previously noted in the vortex distal to a spherical obstruction in a tube (Yu and Goldsmith, 1973). There, it was pointed out that in blood one would expect the concentration of the platelets in the vortex to increase relative to that of the red cells. This argument may well apply to flow in the Y-bifurcations and to that in the partially occluded T-bifurcation.

Finally, it should be noted that in some regions of the spiral vortices (notably during reverse flow) the particles travelled with much reduced velocities (Figures 5, 8 and 10) and were probably subject to much lower shear stresses. During this time, collisions between particles may result in the formation of aggregates, as was found in the case of platelets and polystyrene spheres in the annular vortex at a sudden expansion of vessel diameter (Karino and Goldsmith, 1977). In the case of a partially obstructed branch this could eventually lead to a total occlusion of the lumen. The fact that aggregates of spheres were not observed in the bifurcations is probably due to the use of a non-aqueous suspending medium in which the interaction forces are very

low. It remains to be seen whether the above considerations apply when experiments with red cell and platelet suspensions, as well as whole blood, are carried out.

REFERENCES

ARNOT, R.S., AND LOUW, J.H. (1962). Atheroma of the aortic bifurcation. Brit. Med. J. 3, 470-473.

BEALES, J.S.M., AND STEINER, R.E. (1972). Radiological assessment of arterial branching coefficients. Cardiovascular Res. 6, 181-186.

BRENNER, H. (1966). Hydrodynamic resistance of particles at small Reynolds numbers. Adv. Chem. Eng. (T.B. Drew, J.W. Hoopes, and T. Vermeulen, eds.), pp. 287-438, Academic Press, New York and London.

BRECH, R., AND BELLHOUSE, B.J. (1973). Flow in branching vessels. Cardiovascular Res. 7, 593-600.

CARO, C.G., FITZ-GERALD, J.M., AND SCHROTER, R.C. (1971). Arterial wall shear. Observation, correlation and proposal of a shear dependent mass transfer mechanism for atherogenesis. Proc. Roy. Soc. (London). B 177, 109-159.

COX, R.G., AND HSU, S.K. (1976). The lateral migration of solid particles in a laminar flow near a plane wall. Intern. J. Multiphase Flow (In Press).

FEUERSTEIN, I.A., ELMASRY, O.H., AND ROUND, G.F. (1976). Arterial bifurcation flows — effects of flow rate and area ratio. Can. J. Physiol. Pharmac. 54, 795-808.

FOX, J.A., AND HUGH, A.E. (1966). Localization of atheroma. A theory based on boundary layer separation. Brit. Heart J. 28, 388-399.

FOX, J.A., AND HUGH, A.E. (1970). Static zones in the internal carotid artery: correlation with boundary layer separation and stasis in model flows. Brit. J. Radiol. 43, 370-376.

FRIEDMAN, M.H., O'BRIEN, V.O. AND EHRLICH, L.W. (1975). Calculations of pulsatile flow through a bifurcation. Circ. Res. 36, 277-285.

FRY, D.L. (1968). Acute vascular endothelial changes associated with increased blood velocity gradients. Circ. Res. 22, 165-197.

GEISSINGER, H.D., MUSTARD, J.F., AND ROWSELL, H.C. (1962). The occurrence of microthrombi on the aortic endothelium of swine. Can. Med. Assn. J. 87, 405-408.

GOLDSMITH, H.L. (1972). The flow of model particles and blood cells and its relation to thrombogenesis. In "Progress in Hemostasis and Thrombosis", Vol. 1. (T.H. Spaet, ed.), pp. 97-139, Grune & Stratton, New York.

GOLDSMITH, H.L., AND MARLOW, J. (1972). Flow behavior of erythrocytes. I. Rotation and deformation in dilute suspensions. Proc. Roy. Soc. (London). B 182, 351-383.

GOLDSMITH, H.L., AND MASON, S.G. (1975). Some model experiments in hemodynamics. V. Microrheological techniques. Biorheol. 12, 181-192.

GOSLING, R.G., NEWMAN, D.L., BOWDEN, N.L.R., AND TWINN, K.W. (1971). The area ratio of normal aortic junctions. Aortic configuration and pulse-wave reflection. Brit. J. Radiol. 44, 850-853.

GUTSTEIN, W.H., AND SCHNECK, D.J. (1967). In vitro boundary layer studies of blood flow in branched tubes. J. Atheroscler. Res. 7, 295-299.

HESS, W.R. (1927). Handbuch der normalen und pathologischen Physiologie, Bd. VII, Teil 2, pp. 804-933, Bethe, Berlin.

HUGH, A.E., AND FOX, J.A. (1970). The precise localization of atheroma and its association with stasis at the origin of the internal carotid artery — a radiographic investigation. Brit. J. Radiol. 43, 377-383.

HUNG, T.-K. (1970). Vortices in pulsatile flow. In "Proc. Fifth Intern. Congr. Rheology", Vol. 2. (S. Onogi, ed.), pp. 115-127, Univ. of Tokyo Press & Univ. Park Press.

HUNG, T.-K., AND NAFF, S.A. (1969). A mathematical model of systolic blood flow through a bifurcation. Proc. 8th Intern. Conf. Med. Biol. Engr. no. 20-11.

KARINO, T., AND GOLDSMITH, H.L. (1977). Flow behavior of blood cells and rigid spheres in an annular vortex. Phil. Trans. Roy. Soc. (London). (In Press).

KARNIS, A., GOLDSMITH, H.L., AND MASON, S.G. (1966). The flow of suspensions through tubes. V. Inertial Effects. Can. J. Chem. Eng. 44, 181-193.

KREID, D.K., CHUNG, C.-H., AND CROWE, C.T. (1974). Measurements of the flow of water in a "T" junction by the LDV technique. Paper 74-WA/BIO 1, Bioeng. Div. Winter Annual Meeting, ASME, New York, N.Y.

KWAAN, H.C. HARDING, F., AND ASTRUP, T. (1967). Platelet behavior in small blood vessels in vivo. In "Platelets: their role in Hemostasis and Thrombosis" (Brinkhous et al., eds.), pp. 208-220. Thromb. Diathes. Haemorrh. Suppl. 26, Schattauer, Stuttgart.

LALLEMAND, R.C., BROWN, K.G.E., AND BOULTER, P.S. (1972). Vessel dimensions in premature atheromatous disease of aortic bifurcation. Brit. Med. J. 2, 255-257.

LEE, J.-S., AND FUNG, Y.-C. (1971). Flow in non-uniform small blood vessels. Microvasc. Res. 3, 272-287.

LYNN, N.S., FOX, V.G., AND ROSS, L.W. (1970). Flow patterns at arterial bifurcations. In "Symposium on Recent Developments in Biological Fluid Mechanics" Paper 59d. Amer. Inst. Chem. Eng., New York.

MACAGNO, E.O., AND HUNG, T.-K. (1967). Computational and experimental study of a captive annular eddy. J. Fluid Mech. 28, 43-64.

McDONALD, D.A. (1974). Blood Flow in Arteries p. 984, Williams and Wilkins, Baltimore.

McDOWELL, E.M., AND TRUMP, B.F. (1975). Basic fixation and cytochemistry. Intern. Acad. Path. Meeting, New Orleans, La.

MEISELMAN, H.J., AND COKELET, G.R. (1975). Fabrication of hollow vascular replicas using a gallium injection technique. Microvasc. Res. 9, 182-189.

MITCHELL, J.R.A., AND SCHWARTZ, C.J. (1965). "Arterial Disease" Blackwell, Oxford.

NAJAFI, H., DYE, W.S., JAVID, H., HUNTER, J.A., GOLDIN, M.D., SERRY, C., AND JULIAN, O.C. (1975). Late thrombosis affecting one limb of aortic bifurcation graft. Arch. Surg. 110, 409-412.

ROACH, M.R., SCOTT, S., AND FERGUSON, G.G. (1972). The hemodynamic importance of the geometry of bifurcations in the circle of Willis (glass model studies). Stroke 3, 255-267.

RODKIEWICZ, C.M., AND ROUSSEL, C.L. (1973). Fluid mechanics in a large arterial bifurcation. Trans. ASME, 108-112.

SCHRECK, R.M. (1972). Laminar flow through bifurcations with applications to the human lung. Ph.D. Thesis. Northwestern Univ., Evanston, Ill.

SCHROTER, R.C., AND SUDLOW, M.F. (1969). Flow patterns in models of the human bronchial airways. Resp. Physiol. 1, 341-355.

SEGRÉ, G., AND SILBERBERG, A. (1962). Behaviour of macroscopic rigid spheres in Poiseuille flow. II. Experimental results and interpretation. J. Fluid Mech. 14, 136-157.

SMITH, R.L., BLICK, E.F., COALSON, J., AND STEIN, P.D. (1972). Thrombus production by turbulence. J. Appl. Physiol. 32, 261-264.

SPAIN, D.M. (1966). Atherosclerosis. Scientific American. 215, 49-56.

STEHBENS, W.E. (1959). Turbulence of blood flow. Quart. J. Exp. Physiol. 44, 110-117.

STEHBENS, W.E. (1974). Changes in the cross-sectional area of the arterial fork. Angiology 25, 561-575.

TALUKDER, N. (1975). An investigation on the flow characteristics in arterial branchings. Paper 75 - APMB 4, Conf. Appl. Mech., Symp. Biomech., Troy, N.Y., ASME, New York, N.Y.

TEXON, M., IMPARATO, A.M., AND HELPERN, M. (1965). The role of vascular dynamics in the development of atherosclerosis. J. Amer. Med. Assn. 194, 1226-1230.

YU, S.K., AND GOLDSMITH, H.L. (1973). Behavior of model particles and blood cells at spherical obstructions in tube flow. Microvasc. Res. 6, 5-31.

ZAMIR, M., AND ROACH, M.R. (1973). Blood flow downstream of a two-dimensional bifurcation. J. Theor. Biol. 42, 33-48.

CHAPTER III

Claims to original research

Recommendations for future work

(1) CLAIMS TO ORIGINAL RESEARCH

1) A microscopic flow system, constructed by dissecting, fixing and mounting dog mensetery blood vessels was used to study the flow of rigid spheres $\leq$ 35 μm diameter in small bifurcations resembling those found in man. No flow separation was observed at Reynolds numbers up to 150.

2) Measurements of the vessel dimensions, bifurcation angles and radii of curvature in a number of dog mesentery bifurcations were carried out.

3) The flow behavior of the rigid spheres was also studied in model Y-bifurcations of similar size as those from dog mesentary, but having much smaller radii of curvature on the outer walls and higher area ratios. In these, a pronounced secondary flow, and flow separation at Reynolds numbers > 80 was observed at the entry of the daughter branches.

4) The formation, growth, and flow patterns of the vortex in a partially occluded T-bifurcation was observed as a function of the ratio of flow rates in the daughter branches (degree of occlusion), and as a function of the parent tube Reynolds number.

5) The distribution of rigid spheres in the vortices of the Y- and T-bifurcations were found to depend on particle diameter, the larger spheres being excluded from streamlines originating very close to the tube walls.

(2) RECOMMENDATIONS FOR FUTURE WORK

The present work was but a first step in understanding particle behavior in flow through bifurcations. In order to relate these results further to blood flow in branching vessels of the vasculature, it is felt that the following areas should be investigated in the future:

(1) Further experiments in model Y-bifurcations using suspensions of rigid spheres in which the area ratio is varied between 1.0 and 2.0, at a given bifurcation angle, to determine the effect on secondary flow and the formation of vortices.

(2) The construction of model bifurcation channels set in a material of lower refractive index than Epon, so that the motions of blood cells in their aqueous media can be observed without major optical distortion.

(3) The construction of model bifurcation channels mounted such that it is possible to photograph particle motions not only in the common median plane of parent and daughter branches, as described in this thesis, but also in a direction along the median plane, so as to better characterize motions in the secondary crossflow (e.g. Yu and Goldsmith, 1973; Feuerstein et al. 1976).

(4) Flow experiments using dilute suspensions of human red cells and platelets with the aim of characterizing the behavior and distribution of single cells as well as aggregates (rouleaux and platelet thrombi) in the vortex region. The work should then be extended to examine blood flow at higher hematocrits

in the bifurcation.

References

FEUERSTEIN, I.A., ELMASRY, O.A., AND ROUND, G.F. (1976). Arterial bifurcation flows - effect of flow rate and area ratio. Can. J. Physiol. Pharmacol. 54, 195-208.

YU, S.K., and GOLDSMITH, H.L. (1973). Behavior of model particles and blood cells at spherical obstructions in tube flow. Microvasc. Res. 6, 5-31.

APPENDIX A

Further Details of the Travelling Tube Apparatus

Figure A-1. Photograph of the overall view of the apparatus mounted on a vertically positioned metal base plate. The optical assembly, shown with the microscope tube removed, consists of the high intensity mercury arc A and low intensity tungsten B illuminators, the microscope base C and microscope stand D. Light is conducted along a tube via the condenser, the edge of which is just visible, to the object - the flow tube - which is mounted on the moveable platform I which also supports the infusion syringe whose plunger is driven along a screw thread by the d.c. motor shown at the top via the gear box E.

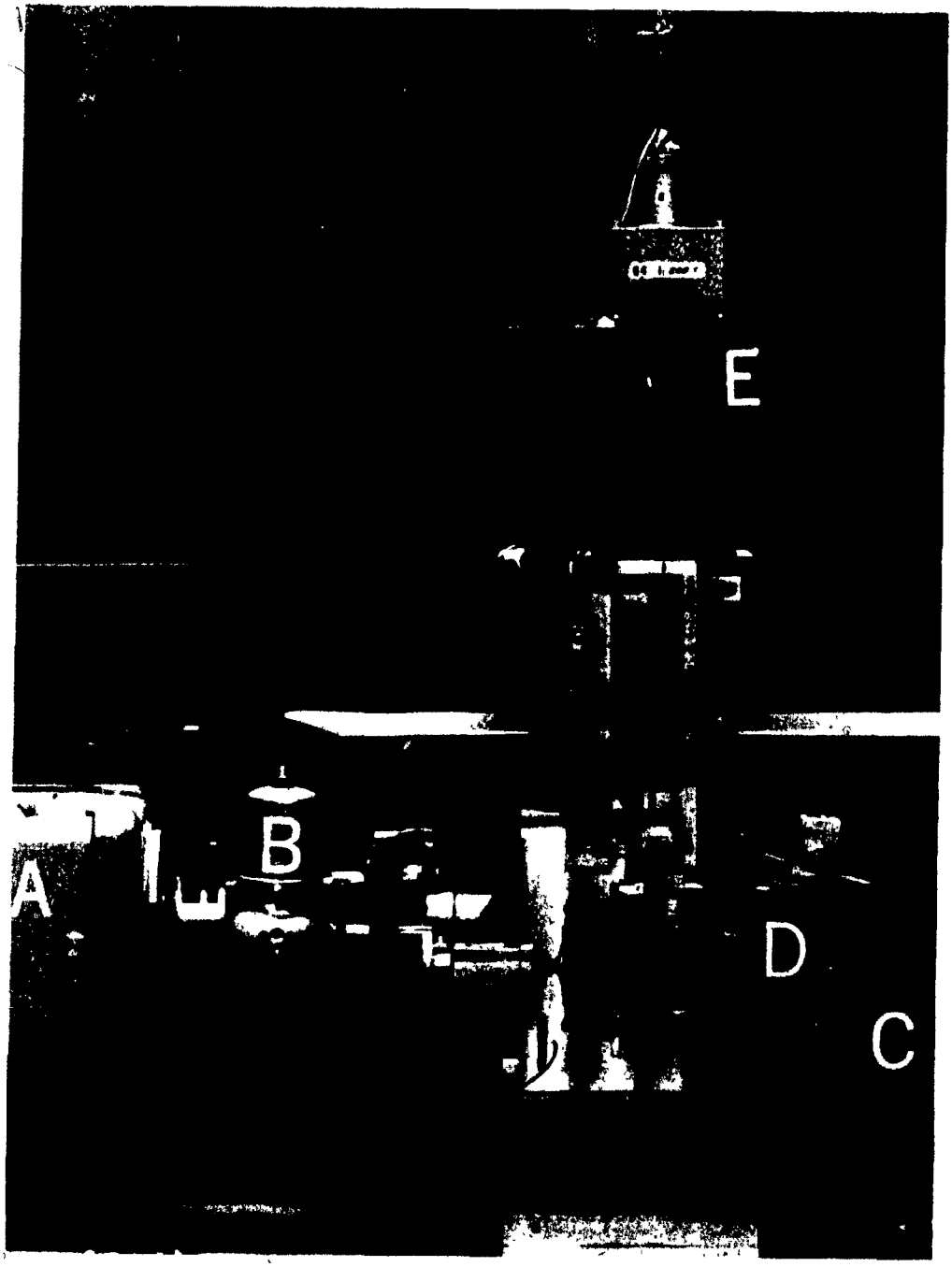
E
A
B
D
C

Figure A-2. Detailed view of the flow system. As in Figure A-1 C denotes the microscope base plate and the microscope tube has been removed in order to show a flow tube which is mounted on a glass slide H held in position by the clamp J. The picture shows the infusion pump plunger G which is moved by the driveshaft F along a screw thread. The syringe is held in position by the plexiglass clamp K and connected to the flow tube via a syringe needle embedded in epoxy resin. The whole assembly is attached to the moveable platform I which is driven up or down by a continuously variable speed d.c. motor. In the present experiments the dog bifurcations were also mounted on glass slides; the model bifurcations, drilled within an epon block were cut to fit within the clamp J, and were connected to the infusion syringe by means of polythene catheter tubes.

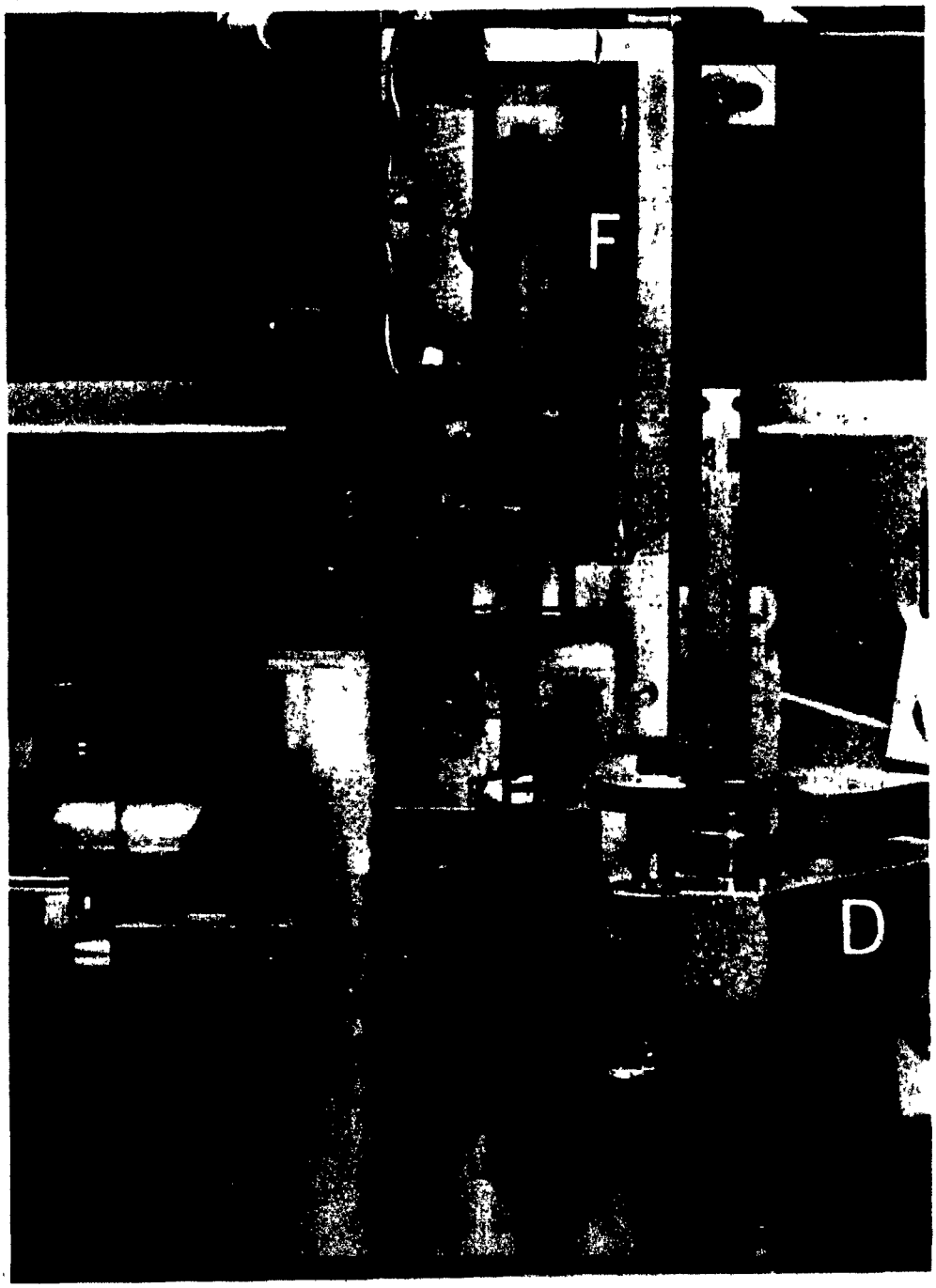
F
D

APPENDIX B

Calculation of radial migration in the entrance tube of a bifurcation

The radial migration of rigid spheres away from the tube wall has been observed at tube Reynolds numbers lower than those used in the present work (Segré and Silberberg, 1962; Karnis et al., 1966) and is due to inertia of the fluid and interaction of the particles with the wall (Cox and Brenner, 1968; Vasseur, 1973; Cox and Hsu, 1976). The rate of migration in Poiseuille flow was found to increase with the particle Reynolds number Re_p (Segré and Silberberg, 1961; 1962)

$$Re_p = \frac{4}{3} b \left(\frac{b}{R_o}\right)^2 . \frac{\rho}{\eta} \bar{U}_o, \qquad \ldots (1)$$

where b is the sphere radius, becoming appreciable at $Re_p > 10^{-4}$. The rates were thus very sensitive to the ratio of particle to tube radius. In the experiments carried out using a T-bifurcation, for 35 μm spheres, Re_p varied from 1.2×10^{-4} to 1.8×10^{-3} and some radial migration would be expected. Measurements with rigid spheres have shown (Segré and Silberberg, 1962) that migration occurs away from the tube center as well as from the wall and that the equilibrium radial position R* at which movement across the lines of flow ceases, is a little more than half way from the tube axis. The rates of migration in this, so called, tubular pinch effect were found to be given by:

$$\frac{dR}{dt} = 0.2 \bar{U}_o \, Re \left(\frac{b}{R_o}\right)^3 . \frac{R}{R_o} \left[1 - \frac{R}{R^*}\right], \qquad \ldots (2)$$

i.e., $dR/dt > 0$ when $R < R^*$ (outward migration) and $dR/dt < 0$ when $R > R^*$ (inward migration).

In order to calculate the inward radial migration of a sphere after travelling an axial distance Δx_o of 20 mm (the entrance length of the T-bifurcation with a radius $R_o = 0.358$ mm), equation (2) is

divided into the equation of motion for Poiseuille flow:

$$U(R) = \frac{dx}{dt} = 2\bar{U}_o\left[1 - \frac{R^2}{R_o^2}\right], \qquad \ldots (3)$$

and then integrated between given limits of radial distance R_1 and R_2. In terms of the dimensionless radial distance $\beta = R/R_o$, one obtains:

$$\Delta x_o = \frac{5\eta}{\rho\bar{U}_o}\left[\frac{R_o}{b}\right]^3 \cdot \left[\ell n \frac{\beta}{1 - \frac{\beta}{\beta^*}} + \beta\beta^* + \beta^{*2}\, \ell n \left(1 - \frac{\beta}{\beta^*}\right)\right]_{\beta = \beta_1}^{\beta = \beta_2} \qquad \ldots (4)$$

where $\beta^* = R^*/R_o$. It can be shown using equation (4) that a 15 μm sphere entering the flow channel at $\beta_1 = 0.979$ (the closest streamline to the tube wall due to the mechanical exclusion of particle centers at radial distances greater than one sphere radius from the tube wall) would migrate 0.4 and 6.8 μm inward to $\beta_2 = 0.978$ and 0.960 at $\bar{U}_o = 12$ and 176 mm sec^{-1} respectively. By contrast, a 32 μm sphere entering the flow channel at $\beta_1 = 0.955$, the closest streamline, would migrate inward 2 μm to $\beta_2 = 0.950$ and 20 μm to $\beta_2 = 0.896$ at the above two flow rates.

REFERENCES

COX, R.G., AND BRENNER, H. (1968). The lateral migration of solid particles in Poiseuille flow. Part I. Theory. Chem Eng. Sci. 23, 147-173.

COX, R.G., AND HSU, S.K. (1976). The lateral migration of solid particles in a laminar flow near a plane wall. Intern. J. Multiphase Flow. (In press).

KARNIS, A., GOLDSMITH, H.L. AND MASON, S.G. (1966). The flow of suspensions through tubes. V. Inertial effects. Canad. J Chem. Eng. 44, 181-193.

SEGRÉ, G., AND SILBERBERG, A. (1961). Radial particle displacements in Poiseuille flow of suspensions. Nature (London) 189, 209-210.

SEGRÉ, G., AND SILBERBERG, A. (1962). Behavior of macroscopic rigid spheres in Poiseuille flow. II. Experimental results and interpretation. J. Fluid Mech. 14, 136-157.

VASSEUR, P. (1973). The lateral migration of spherical particles in a fluid bounded by parallel plane walls. Ph.D. Thesis, McGill University, Montreal, Canada.